Zeitschrift: IABSE reports of the working commissions = Rapports des commissions de travail AIPC = IVBH Berichte der Arbeitskommissionen

Band: 29 (1979)

Rubrik: Session II: Beams and shear walls

SESSION II

Beams and Shear Walls

Poutres et voiles soumis à l'effort tranchant

Träger und Schubwände

Chairman: Prof. D.H. Clyde, Australia

Introductory Lectures: „Plastic Analysis of Reinforced Concrete Shear Walls"
P. Marti, Switzerland

„Plastic Analysis of Reinforced Concrete Beams"
Prof. B. Thürlimann, Switzerland

(The Introductory Lectures are published in the Introductory Report, Volume AK 28)

Leere Seite
Blank page
Page vide

II

Plastic Solutions for Reinforced Concrete Beams in Shear

Solutions plastiques pour des poutres en béton armé soumises à un effort tranchant

Plastizitätstheoretische Lösungen für schubbeanspruchte Stahlbetonbalken

J.F. JENSEN
Civil Engineer, M.Sci.Eng.
Technical University of Denmark
Lyngby, Denmark

SUMMARY
The paper treats reinforced concrete beams in shear by means of the theory of plasticity. Disregarding the tensile strength of the concrete, exact solutions are found for some common cases of beams and loading, and comparison is made with test results. Furthermore, an upper-bound analysis is carried out to investigate the influence of the tensile strength of the concrete in beams without shear reinforcement.

RESUME
La théorie de la plasticité est appliquée pour l'analyse des poutres en béton armé soumises à un effort tranchant. La résistance à la traction du béton étant supposée négligeable, quelques solutions complètes sont établies et des comparaisons avec des résultats expérimentaux sont faites. L'influence de la résistance à la traction du béton sur la charge ultime de poutres sans armature de cisaillement est examinée par la méthode cinématique.

ZUSAMMENFASSUNG
Durch Querkraft beanspruchte Stahlbetonbalken werden mit der Plastizitätstheorie behandelt. Unter der Annahme einer verschwindenden Betonzugfestigkeit werden vollständige Lösungen für einige übliche Fälle angegeben, und Vergleiche mit Versuchsergebnissen werden durchgeführt. Der Einfluss der Betonzugfestigkeit auf die Traglast von Balken ohne Schubbewehrung wird mit der kinematischen Methode untersucht.

1. INTRODUCTION

This paper presents briefly a number of plastic solutions for determination of the shear strength of reinforced concrete beams. For the detailed examination, the reader is referred to [4].

2. BASIC ASSUMPTIONS

The solutions presented are based on the following assumptions:
- The concrete is a rigid, perfectly plastic material with Coulombs modified failure hypothesis as its yield criterion. The angle of friction is φ, the uniaxial compression strength is f_c^*, and the tensile strength $f_t^* = \rho f_c^*$. The deformations are governed by the normality condition.
- The reinforcing steel is rigid, perfectly plastic, and can only resist forces in its longitudinal direction. The magnitude of the yield stress is the same for tension as for compression.
- The stress field in the beam is plane.

3. SOME EXACT SOLUTIONS

In the solutions in this section it is assumed that the concrete has no tensile strength, i.e., that $f_t^* = 0$. Regarding the consequences of this assumption, see section 4.

3.1 Stringer beam with shear reinforcement - concentrated load.

Plastic solutions for this type of beam and load, see fig. 1, have been known for some years, [1] and [2]. However, none of these works give coinciding upper-bound and lower-bound solutions for beams with very little shear reinforcement, which is a somewhat unsatisfactory state of affairs. It will be shown here how the desired coincidence can be obtained by quite a simple alteration of the stress distribution on which lower-bound solutions known so far are based.

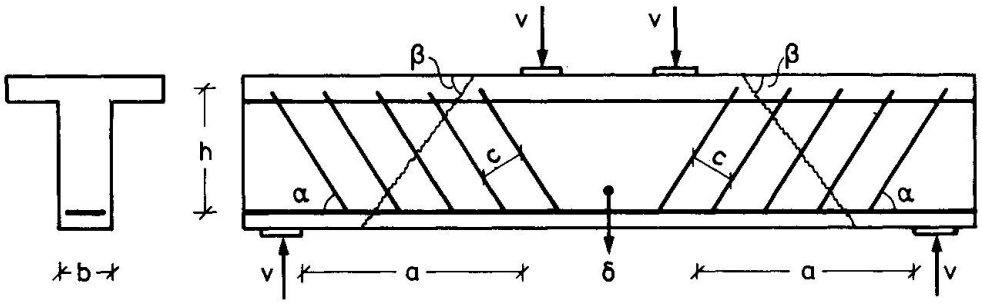

Fig. 1. Beam under consideration, showing failure mechanism.

In the following, the compression zone and the tensile reinforcement are idealized as stringers, and these are at the same time assumed to be sufficiently strong to resist the stringer forces occurring.

Furthermore, the stirrups, which are all inclined at the angle α with the beam axis, are assumed to be placed so closely together that the stirrup forces can be substituted by a uniformly distributed equivalent stirrup stress.

Let us now consider the part of the beam located between the loading plate and the support, with the distribution of the concrete stresses in the beam web shown in fig. 2. Here, the best lower-bound is obtained by optimizing the angle θ, putting

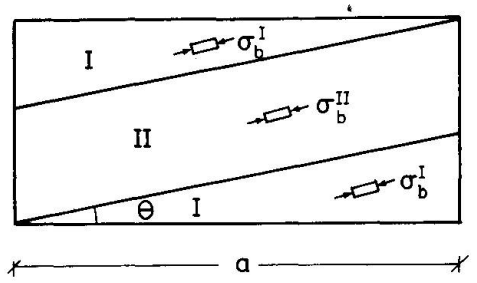

Fig. 2. Stress field in concrete with low degree of reinforcement.

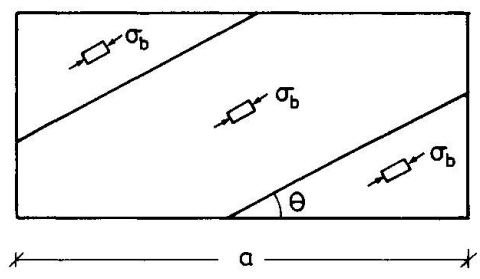

Fig. 3. Stress field in concrete with high degree of reinforcement.

$\sigma_b^{II} = f_c^*$ and assuming yielding of the shear reinforcement. The solution found in this way is valid as long as σ_b^I together with the equivalent stirrup stress fulfil the boundary conditions along the stringers without exeeding the uniaxial compression strength of the concrete, f_c^*. With the stress distribution applied, this is possible as long as

$$\psi \le \psi' = \frac{\sqrt{1+(\frac{a}{h})^2} - \frac{a}{h}}{2\sin^2\alpha\sqrt{1+(\frac{a}{h})^2}} \qquad \psi = \frac{A_s f_{ys}}{b\,c\,f_c^*} \tag{3.1}$$

Here, we have introduced the mechanical degree of shear reinforcement, ψ. A_s denotes the stirrup area crossing the concrete area $b \cdot c$, c is the spacing between the stirrups measured at right angles to these, and finally f_{ys} is the yield stress of the stirrup reinforcement.

In case of larger degrees of shear reinforcement than given by (3.1), the stress distribution from fig. 2 must be replaced by that shown in fig. 3. Here, we put $\sigma_b = f_c^*$, and for a given equivalent stirrup stress, the angle θ is determined such that the boundary conditions slong the stringers is fulfilled in all zones shown. The equivalent stirrup stress is then optimized, leading to yielding of the shear reinforcement as long as

$$\psi \le \psi'' = \frac{1+\cos\alpha}{2\sin^2\alpha} \tag{3.2}$$

while the best lower-bound is obtained without yielding of the shear reinforcement, when $\psi \ge \psi''$.

The complete result of the lower-bound solution can be written as follows:

$$\frac{\tau}{f_c^*} = \frac{V}{b\,h\,f_c^*} = \tfrac{1}{2}\left(\sqrt{1+(\tfrac{a}{h})^2} - \tfrac{a}{h}\right) + \psi\sin^2\alpha\left(\tfrac{a}{h} + \cot\alpha\right), \quad \psi \le \psi' \tag{3.3}$$

$$\frac{\tau}{f_c^*} = \sqrt{\psi\sin^2\alpha(1-\psi\sin^2\alpha)} + \psi\sin\alpha\cos\alpha, \quad \psi' \le \psi \le \psi'' \tag{3.4}$$

$$\frac{\tau}{f_c^*} = \tfrac{1}{2}\cot\frac{\alpha}{2}, \quad \psi'' \le \psi \tag{3.5}$$

The solution determined by means of (3.3) - (3.5) is exact, because an upper-bound solution derived on the basis of the failure mechanism from fig. 1 gives the same carrying capacity when the angle β is optimized.

Fig. 4 shows the results of 84 shear tests on simple T-beams with vertical stirrups, carried out in the years 1967 to 1975 at the Structural Research Laboratory of the Technical University of Denmark, compared with the theory. In the diagram, an empirical expression from [1] is used for determining the apparent strength of the concrete in the beam web on the basis of a given cylinder compression strength, valid for stringer beams with shear reinforcement:

$$f_c^* = (0.8 - \frac{f_c}{200}) \cdot f_c \qquad (3.6)$$

In (3.6), both f_c^* and f_c are measured in MPa, f_c denoting the cylinder strength.

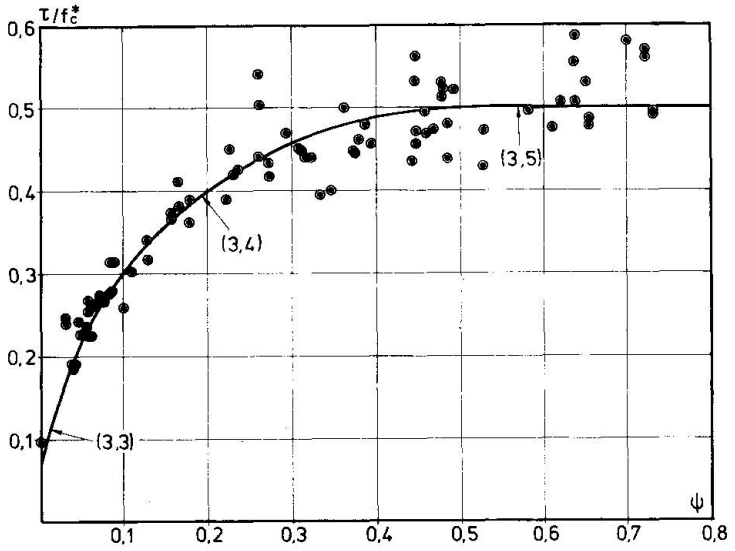

Fig. 4.
Comparison of the theory and the results of tests.

3.2 Rectangular beam without shear reinforcement - uniformly distributed load.

We now consider a simply supported beam with the free span 2a, see fig. 5. It is assumed that the force, T, in the tensile reinforcement can be transmitted to the concrete by the part of the beam lying behind the support, as shown, in principle, in the figure.

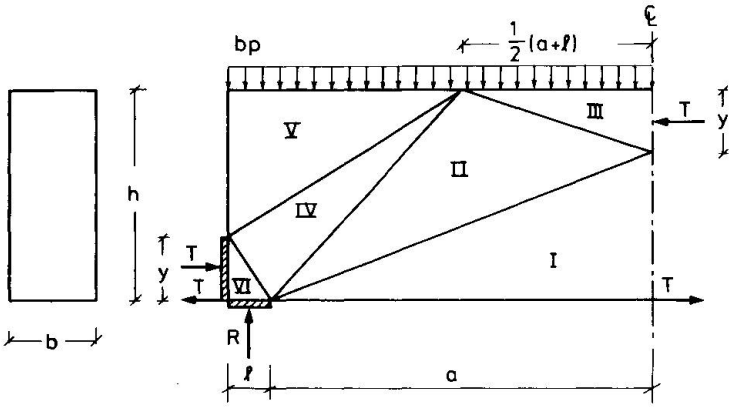

Fig. 5. Beam under consideration showing adopted division of concrete into zones with homogeneous stress fields.

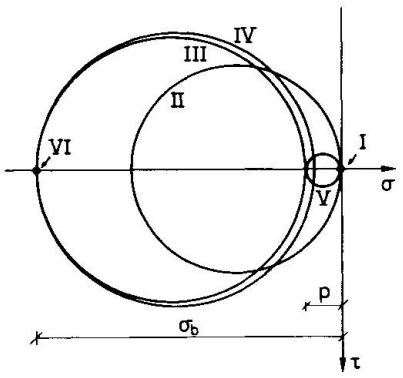

Fig. 6. Mohr's circles for the stress fields in the zones from fig. 5.

The concrete is divided into zones with homogeneous stress fields, as shown in fig. 5. The stress fields are illustrated by means of the Mohr's circles in fig. 6. As seen, the length ℓ is determined such that hydrostatic pressure is obtained in zone VI. No tensile stresses occur in any part of the concrete, and in the best solution, the largest compression stress, σ_b, is obtained simultaneously in zones III, IV and VI. We put $\sigma_b = f_c^*$, giving the magnitude of y, and the solution then becomes:

$$\frac{\tau}{f_c^*} = \frac{p\,a}{h\,f_c^*} = \frac{2\Phi(1-\Phi)\frac{a}{h}}{(\frac{a}{h})^2 + 2\Phi(1-\Phi)} \quad , \quad \Phi = \frac{A_\ell\, f_{y\ell}}{b\,h\,f_c^*} \leq \tfrac{1}{2} \qquad (3.7)$$

$$\frac{\tau}{f_c^*} = \frac{\frac{a}{h}}{2\left(\frac{a}{h}\right)^2 + 1} \qquad \Phi \geq \tfrac{1}{2} \qquad (3.8)$$

where we have introduced the mechanical degree of longitudinal reinforcement, Φ. A_ℓ is the cross-sectional area of the reinforcement, and $f_{y\ell}$ is the yield stress of the same. In opposition to (3.7), no yielding of the reinforcement occur corresponding to (3.8).

The solution given by (3.7) and (3.8) is exact, since an upper-bound solution based on the failure mechanism from fig. 7 leads to the same carrying capacity. The points A and B act as hinges, and part I rotates an angle θ about the point A. Part II's displacement is a pure translation.

Fig. 8 shows a comparison of the results obtained in theory and those obtained from tests for a narrow interval of degrees of reinforcement. A detailed analysis of the test results versus theory has not yet been performed. Therefore, since the apparent concrete strength will presumably vary in relation to the cylinder compression strength, analogously to (3.6), we have chosen only to consider a number of tests with concrete strengths that do not vary too much in relation to each other. We have then tentatively put $f_c^* = 0.65\ f_c$.

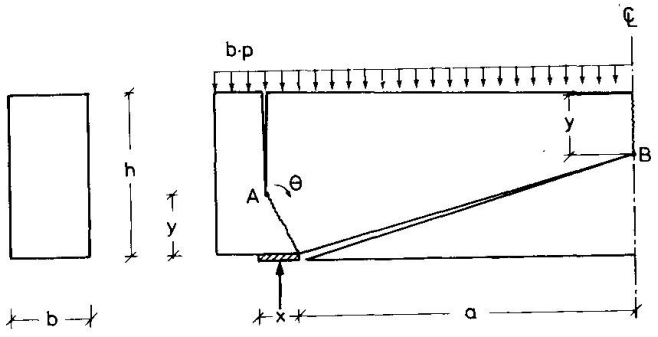

Fig. 7. Failure mechanism used.

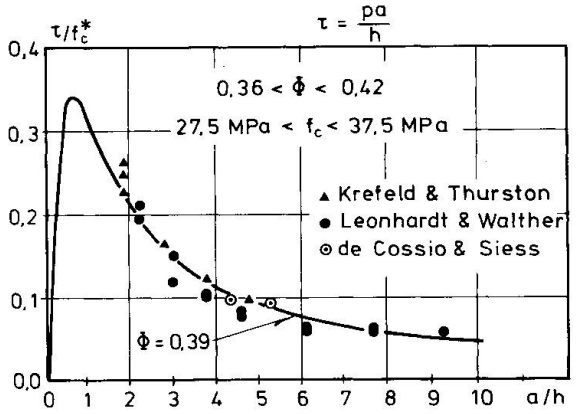

Fig. 8. Comparison with tests from the literature.

With regard to the type of load and beam considered here, it is also interesting to compare the carrying capcitites measured in tests reported in the literature with the flexural strength determined in accordance with the CEB-FIP Model Code. In a comparison of this nature reported in [1] and [3] for a total of 115 tests, the average value of the ratio between the two carrying capacities is found to be 1.00, with a coefficient of variation of 15.2%. Thus, apart from ensuring a ductile failure, only little can generally be gained by reinforcing with stirrups.

3.3 Rectangular beam without shear reinforcement - combined central, normal force and concentrated load.

For derivation of the lower-bound solution, use is made of the stress distribution shown in fig. 9. Forces in the tensile reinforcement are assumed to be transmitted to the concrete behind the support, as in case of the beam in section 3.2.

The corresponding upper-bound is derived on the basis of a failure mechanism analogous to that shown in fig. 7., see fig. 10. The best solution is found by optimizing x, y_1 and y_2.

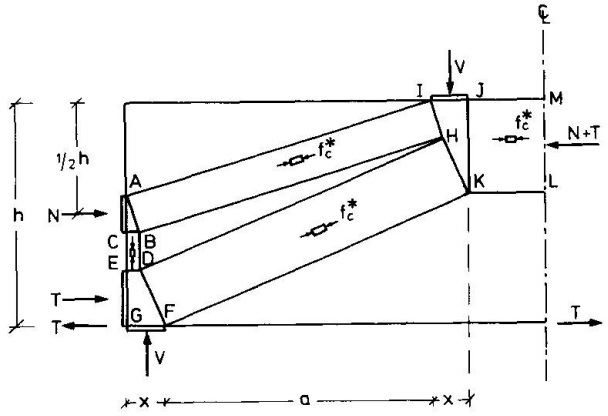

Fig. 9. Stress distribution for use in lower-bound solution.

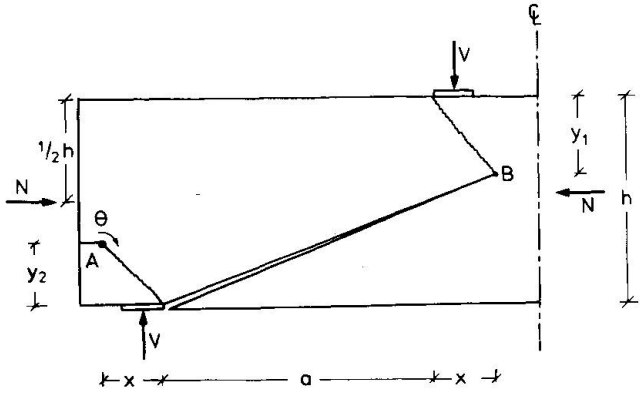

Fig. 10. Sketch showing failure mechanism used.

Both the lower-bound and the upper-bound solution leads to the carrying capacities:

$$\frac{\tau}{f_c^*} = \frac{V}{b\,h\,f_c^*} = \tfrac{1}{2}\left(\sqrt{2\pi(1-\pi-2\Phi)+4\Phi(1-\Phi)+\left(\frac{a}{h}\right)^2}-\left(\frac{a}{h}\right)\right), \quad 0 \le \pi \le 1-2\Phi \qquad (3.9)$$

$$\frac{\tau}{f_c^*} = \tfrac{1}{2}\left(\sqrt{1-\pi^2+\left(\frac{a}{h}\right)^2}-\frac{a}{h}\right), \quad 1-2\Phi \le \pi \le 1 \qquad (3.10)$$

where we have introduced the dimensionless parameter, π, by $N = \pi\, b\, h\, f_c^*$, and the degree of longitudinal reinforcement, Φ, from (3.7). Only corresponding to (3.9), yielding of the reinforcement is obtained.

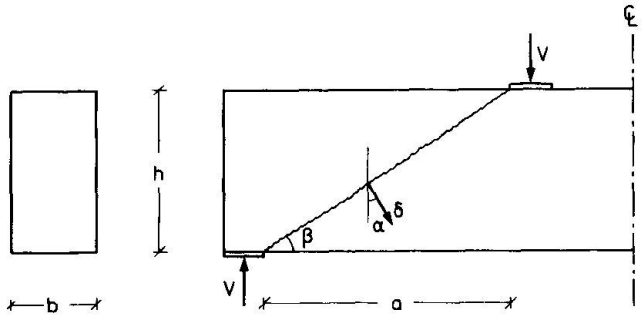

Fig. 11. Alternative failure mechanism for $\pi = 0$.

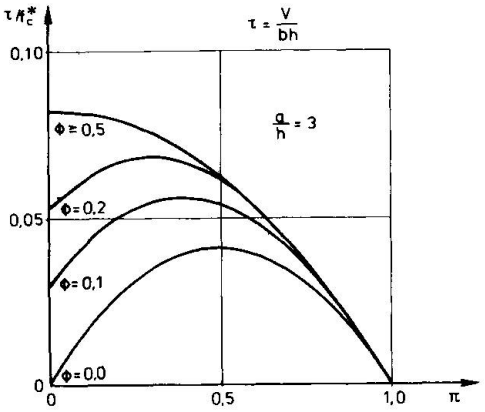

Fig. 12. Variation of carrying capacity with Φ and π.

Now, compare the failure mechanism from fig. 10 with that from fig. 11. When the beam is not subjected to a normal force, the mechanism from fig. 11 leads when α is optimized to the same carrying capacity as given by (3.9) - (3.10) for $\pi = 0$. Here α denotes the angle between the vertical and the relative displacement, δ, between zones I and II. In this case, the solution is well known, and comparisons with tests have previously been performed, cf. [1] and [3].

For $\pi \neq 0$, the solution has not yet been verified by tests, so in fig. 12 only the theoretical relationship between the carrying capacity and a couple of the main parametres is shown. The variation with the relative shear span, $\frac{a}{h}$, is analogous to that shown in fig. 14 for $\rho = 0$.

4. UPPER-BOUND ANALYSIS OF THE EFFECT OF TENSILE STRENGTH

In beams provided with shear reinfrocement, the concrete in the beam web will be completely cracked all the way through before failure occurs, so the concrete cannot be assumed to have any tensile strength in a determination of the carrying capacity. Therefore, in this section only beams without shear reinforcement will be considered, since the cracking here will be less pronounced, which means that the concrete can reasonably be assumed to have a certain, although minimum, tensile strength.

4.1 Rectangular beam without shear reinforcement - concentrated load.

The failure mechanism shown in fig. 13 is chosen as the basis for the upper-bound solution. At failure, the middle part of the beam undergoes the relative displacement, δ, vertically downwards in relation to the parts of the beam over the supports, since we will only consider beams with such strong longitudinal reinforcement that yielding will not occur in this. The failure line adopted is straight in all cases, which is also shown by variational analysis to be the optimum form. The best upper-bound solution is obtained by optimizing the angle β.

The solution arrived at is illustrated in fig. 14, where it should be noted that the hereby calculated shear capacity becomes independent of the shear span when this exeeds a certain limit, even though the concrete is only assumed to have a rather low tensile strength. This indicates, as is well known, that if the shear span is sufficiently long, then another failure mechanism, the flexural failure, must be more dangerous than the shear failure.

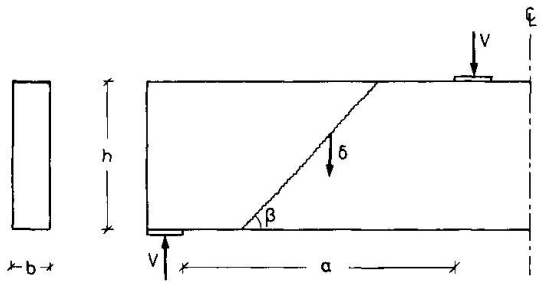

Fig. 13. Failure mechanism.

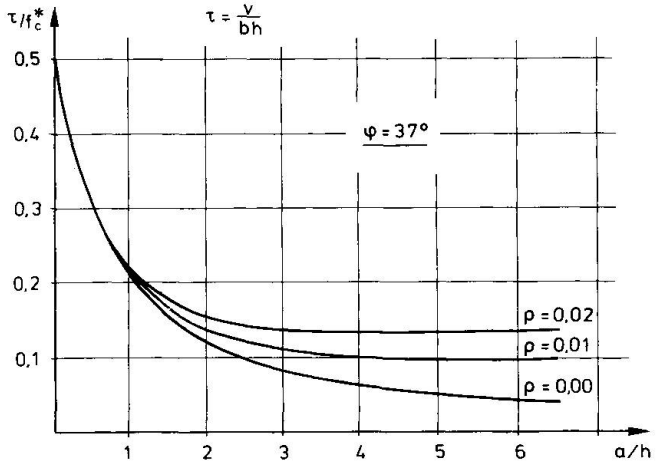

Fig. 14. Variation of shear capacity with ρ and $\frac{a}{h}$. $f_t^* = \rho f_c^*$.

If this had been a stringer beam with sufficiently strong stringers, the solution illustrated in fig. 14 would be exact, since in this case a corresponding lower-bound solution is found in [4].

4.2 Rectangular beam without shear reinforcement - uniformly distributed load.

Generalizing the failure mechanism from fig. 7 to that shown in fig. 15 for a beam with such strong longitudinal reinforcement that yielding of this will not occur, we find by optimation that $y = \frac{1}{2}h$ and $x_1 = 0$. The best value for x_2 and d for use in the following has been calculated numerically. The results are shown in fig. 16 and 17.

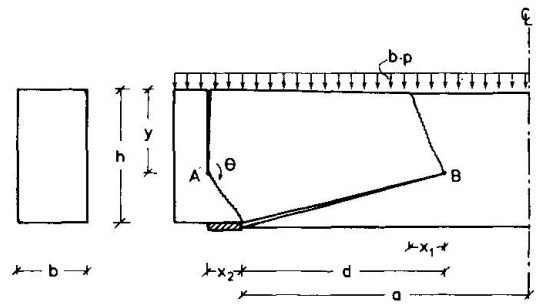

Fig. 15. Failure mechanism.

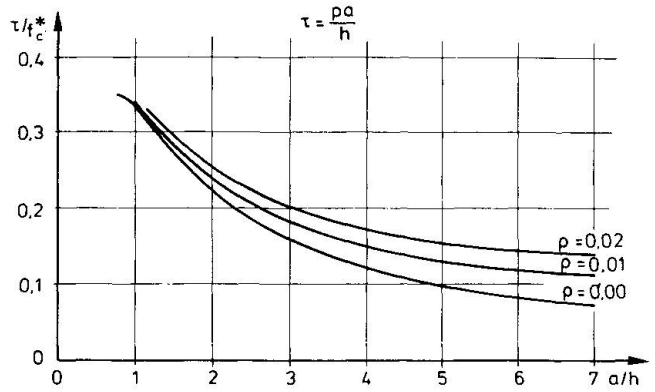

Fig. 16. Variation of carrying capacity with ρ and $\frac{a}{h}$.

Fig. 17. Example of geometry of failure pattern at $\frac{a}{h} = 3$.

Note from fig. 17 how the compression failures in the top of the beam move out towards the supports, when the tensile strength is taken into account.

REFERENCES

[1] Nielsen, M.P., M.W. Bræstrup, B.C. Jensen and F. Bach:"Concrete Plasticity". Dansk Selskab for Bygningsstatik. Special Publication. Copenhagen, 1978.

[2] Thürlimann, B.:"Plastic Analysis of Reinforced Concrete Beams". IABSE Colloquium, Copenhagen, 1979. Introductory Report, pp. 71-90.

[3] Roikjær, M., C. Pedersen, M.W. Bræstrup, M.P. Nielsen og F. Bach: "Bestemmelse af ikke-forskydningsarmerede bjælkers forskydningsbæreevne". Rapport Nr. I 62, Afdelingen for Bærende Konstruktioner, Danmarks tekniske Højskole, 1978.

[4] Jensen, J.F., M.W. Bræstrup, F. Bach og M.P. Nielsen:"Nogle plasticitetsteoretiske bjælkeløsninger". Rapport Nr. R 101, Afdelingen for Bærende Konstruktioner, Danmarks tekniske Højskole, 1978.

II

Shear in Beams with Bent-Up Bars

L'effort tranchant dans les poutres avec des barres relevées

Schub in Balken mit aufgebogener Bewehrung

C. PEDERSEN
Ph. D. Student
Technical University of Denmark
Copenhagen Lyngby, Denmark

SUMMARY
The shear strength of reinforced concrete beams with bent-up bars as shear reinforcement is analysed by means of the upper bound theorem of the theory of plasticity. The upper bound solutions are compared with the results from a number of tests and good agreement is found.

RESUME
La résistance au cisaillement de poutres en béton armé avec des barres relevées est examinée par la méthode cinématique de la théorie de la plasticité. Les valeurs extrêmes de la charge ultime sont comparées avec les résultats d'essais et une bonne concordance peut être constatée.

ZUSAMMENFASSUNG
Der Schubwiderstand von Stahlbetonbalken mit aufgebogenen Stäben als Schubbewehrung wird mit der kinematischen Methode der Plastizitätstheorie untersucht. Die oberen Grenzwerte für die Traglasten werden mit Ergebnissen einer Anzahl von Versuchen verglichen, und eine gute Übereinstimmung wird festgestellt.

1. INTRODUCTION

The purpose of this investigation was to show the usability of the theory of plasticity on this type of problem. In previous examinations by K.W. Johansen and H.C. Sørensen it has been claimed that the contribution of bent-up bars to the shear strength is independent of the inclination of the bar at the bending point. (c.f. [57.1] and [72.1]). Furthermore, in these examinations (in which a model with fixed concrete strut inclination is used) it is claimed that the contribution of the bent-up bars to the shear strength of the beam is usually over-estimated by 41%. However, no failures due to this have been found. It is thus reasonable to ask if the plastic model for shear in reinforced concrete (c.f. [78.2] and [75.1]) gives a more precise description of the problem. This paper is a short version of a similar paper in Danish, [78.3], which gives a more profound description of the analysis.

2. BASIC ASSUMPTIONS

The reinforcing steel and the concrete are both assumed to be rigid, perfectly plastic. The yield locus of the concrete in plane stress is shown in Fig. 1. The associated flow rule is assumed to be valid. The state of stresses in the beam is assumed to be plane. f_c^* denotes the effective concrete strength and is related to the uniaxial compression strength by the equation

$$f_c^* = \nu f_c \qquad (1)$$

ν is a positive figure less than 1 which takes into account that the basic assumptions are never fulfilled in practice, that is, the concrete has not an unlimited capacity of deformation under constant stress and the state of stress is never quite plane.

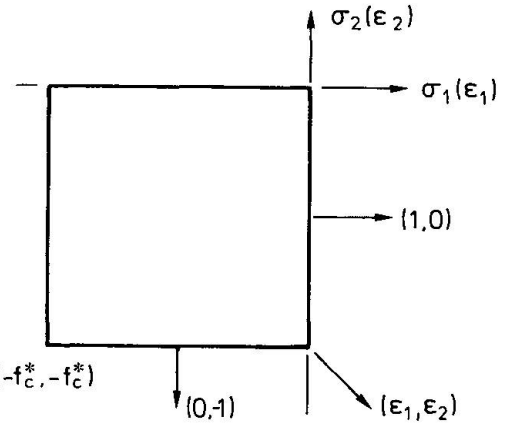

Fig. 1 Yield Locus for Concrete in Plane Stress.

3. THEORETICAL UPPER BOUND SOLUTIONS

The beam in Fig. 2 with only one bent-up bar in the shear span is considered.

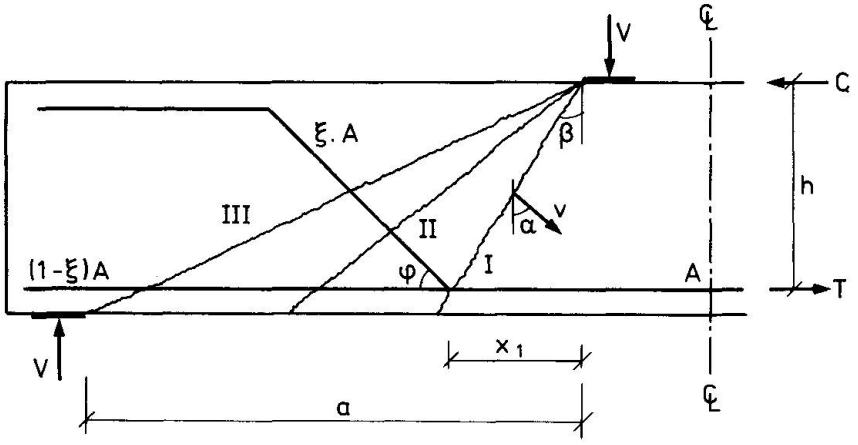

Fig. 2 Failure Mechanisms for Beams with only one Bent-up Bar.

For the failure mechanism corresponding to yield line II it is easy to calculate the external work and the internal work (dissipation) using the basic assumptions (c.f. [78.2]). The following upper-bound solution is obtained by putting the external work equal to the internal work.

$$\frac{\tau}{f_c} = \tfrac{1}{2}\nu\left(\sqrt{1+tg^2\alpha}\cdot\sqrt{1+tg^2\beta} - tg\,\alpha - tg\,\beta\right) + \phi(1-\xi+\xi\cos\varphi) + \xi\,\phi\sin\varphi \qquad (1)$$

The angles α and β are found by minimizing (1). This yields the following values

$$tg\,\beta = a/h \qquad (2)$$

$$\sin\alpha_o = \begin{cases} \dfrac{\frac{1}{2}\nu - \Gamma}{\frac{1}{2}\nu\sqrt{1+tg^2\beta}} & \text{for } \Gamma \le \dfrac{\nu}{2} \\ 0 & \text{for } \Gamma > \dfrac{\nu}{2} \end{cases} \qquad (3)$$

The reduced degree of longitudinal reinforcement is given by

$$\Gamma = \phi(1-\xi+\xi\cos\varphi) \qquad (4)$$

For yield line I similar results can be obtained. In this case $\Gamma = \phi$ and $tg\,\beta = x_1/h$.

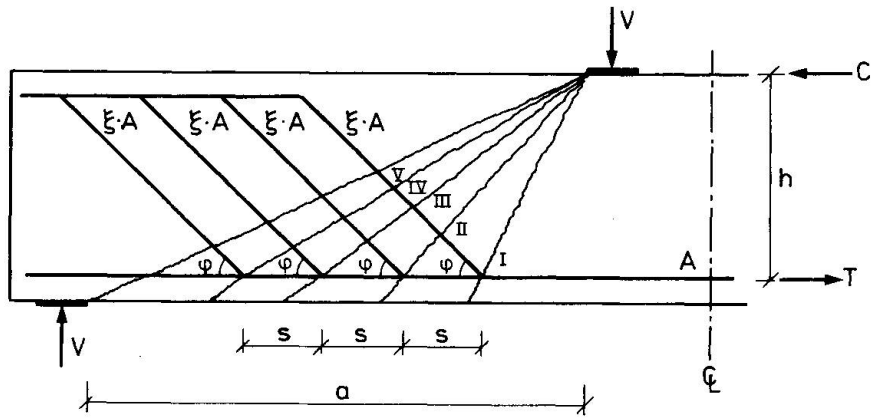

Fig. 3 Failure Mechanisms for a Beam with several Bent-up Bars.

Fig. 3 shows a beam with several bent-up bars in the shear span. This beam has to be investigated for each yield line I, II, III, IV and V. The investigations are carried out using (1) to (4) with varying values of $tg\,\beta$, ξ and Γ.

Alternatively, this beam is analysed by means of the usual expression for the shear strength of a beam with inclined stirrups as shear reinforcement. The shear strength is then given by

$$\frac{\tau}{f_c} = \begin{cases} \dfrac{\nu}{2}\left(\sqrt{1+\lambda^2} - \lambda\right) + \psi\sin^2\varphi\,(\lambda+\cot\varphi) & , \quad 0 \le \psi \le \psi_o \\ \sqrt{\psi\sin^2\varphi\,(\nu-\psi\sin^2\varphi)} + \psi\cos\varphi\sin\varphi & , \quad \psi_o \le \psi \le \dfrac{\nu}{2}\dfrac{1+\cos\varphi}{\sin^2\varphi} \\ \dfrac{\nu}{2}\cot\dfrac{\varphi}{2} & , \quad \psi \ge \dfrac{\nu}{2}\dfrac{1+\cos\varphi}{\sin^2\varphi} \end{cases} \qquad (5)$$

where

$$\psi = \frac{\xi\,A\,f_y}{b\,s\,f_c\sin\varphi} \qquad \text{and} \qquad \psi_o = \frac{\nu}{2}\frac{\sqrt{1+\lambda^2}-\lambda}{\sin^2\varphi\sqrt{1+\lambda^2}} \qquad (6)$$

Finally, a beam with combined stirrups and bent-up bars as shear reinforcement is considered.

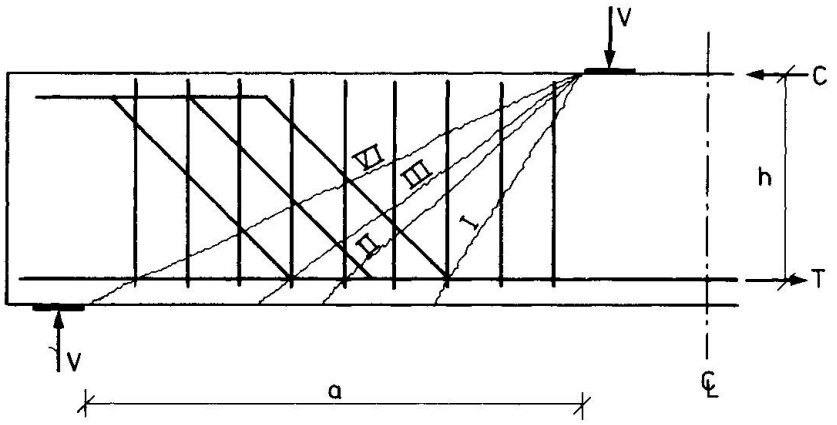

Fig. 4 Reinforced Beam with Stirrups and Bent-up Bars.

For the failure mechanism corresponding to yield line I the following expression for the shear force at failure is found

$$V = n A_s f_{ys} + A f_y \operatorname{tg}\alpha + \tfrac{1}{2}\nu f_c \frac{1-\sin(\alpha+\beta)}{\cos\alpha \cos\beta} \qquad (7)$$

From (7) it is seen that the contribution of the stirrups to the shear force is independent of α. This means that α_o has to be determined as previously.

4. COMPARISON BETWEEN CALCULATED RESULTS AND RESULTS OBTAINED BY TESTS

In this section, a comparison between results calculated by the preceeding upper-bound solutions and results obtained by tests is drawn.

The results from the tests have all been found in the literature. The values of ν have all been determined so that accordance between theory and test was obtained. Finally, these values of ν are compared with the values recommended in [78.2].

4.1 Tests by K. Özden and K.W. Johansen

In [67.1], 4 tests with beams with bent-up bars and 2 tests on beams with combined stirrups and bent-up bars are described. The beam T-11 has been omitted from the present analysis because this beam showed typical brittle failure.

BEAM	h	b	f_c	ϕ	α_o	tg β	τ/f_c	$(\tau/f_c)_E$
	m	m	MPa				ν=0.60	
T5	0.2902	0.110	34.0	0.523	0°	1.29	0.103	0.133
T12	0.2744	0.110	34.0	0.549	0°	0.820	0.142	0.151
T16	0.2672	0.160	34.0	0.416	0°	0.468	0.191	0.113

Table 4.1.1 Calculated and Measured Results (ν = 0.60)

For the beams T-13 and T-14, the following results are found.

BEAM	h	b	f_c	ϕ	α_o	tg β	τ/f_c	$(\tau/f_c)_E$
	m	m	MPa				ν=0.70	
T13	0.2718	0.110	31.1	0.610	0°	0.828	0.177	0.165
T14	0.2714	0.110	31.1	0.627	0°	2.045	0.120	0.129

Table 4.1.2 Calculated and Measured Results (ν = 0.70)

4.2 Tests by F. Leonhardt and R. Walter

The results from 3 tests carried out by F. Leonhardt and R. Walter are described in [63.1]. One of the beams showed flexural failure and is omitted in this analysis.

Strain measurements on the bent-up bars in the tests in [67.1] and [63.1] indicate that no yielding has occured in these before failure. It is therefore reasonable to assume that the yield line runs from the edge of the loading plate to the first bending point of the longitudinal reinforcement.

BEAM	h	b	f_c	ϕ	α_o	tg β	τ/f_c	$(\tau/f_c)_E$
	m	m	MPa				ν=0.75	
TA5	0.335	0.160	19.0	1.433	0^o	0.716	0.235	0.227
TA17	0.345	0.160	25.2	0.777	0^o	0.406	0.253	0.248

Table 4.2.1 Calculated and Measured Results (ν = 0.75)

4.3 Tests by K. Leksukhum and R. Smith

K. Leksuhkum and R. Smith [71.1] have carried out a number of tests on beams with different types of web reinforcement. Here, the tests with bent-up bars are analysed by means of (11) and the following results are found.

BEAM	λ	ψ_o	f_c	ρf_y	ψ	τ/f_c	$(\tau/f_c)_E$	ν
		ν=0.70	MPa	MPa		ν=0.70		
BI-1	2.60	$4.67 \cdot 10^{-2}$	22.8	1.12	$4.91 \cdot 10^{-2}$	0.1533	0.150	0.666
BI-2	2.63	$4.57 \cdot 10^{-2}$	23.6	1.12	$4.75 \cdot 10^{-2}$	0.1505	0.136	0.554
BI-3	2.60	$4.67 \cdot 10^{-2}$	24.8	1.12	$4.52 \cdot 10^{-2}$	0.1463	0.141	0.639
BI-4	2.70	$4.36 \cdot 10^{-2}$	23.6	1.12	$4.75 \cdot 10^{-2}$	0.1505	0.146	0.653
BI-5	2.88	$3.87 \cdot 10^{-2}$	20.9	1.12	$5.36 \cdot 10^{-2}$	0.1611	0.163	0.719
BI-6	2.91	$3.80 \cdot 10^{-2}$	24.7	1.12	$4.53 \cdot 10^{-2}$	0.1465	0.150	0.739
BI-7	2.34	$5.63 \cdot 10^{-2}$	24.4	1.40	$5.74 \cdot 10^{-2}$	0.1675	0.181	0.837
BI-8	2.34	$5.63 \cdot 10^{-2}$	22.6	1.40	$6.19 \cdot 10^{-2}$	0.1748	0.212	1.090
BI-9	3.00	$3.59 \cdot 10^{-2}$	23.6	0.70	$2.97 \cdot 10^{-2}$	0.1162	0.114	0.675
BII-11	2.72	$4.30 \cdot 10^{-2}$	23.4	0.86	$3.68 \cdot 10^{-2}$	0.1307	0.146	0.871

Table 4.3.1 Calculated and Measured Results

4.4 Tests by P. Regan and M.H. Khan

In [71.2], two series of tests by P. Regan and M.H. Khan are described. Series A had both stirrups and bent-up bars as web reinforcement, while series K had only bent-up bars as web reinforcement. The results are shown in Table 4.4.1 which is shown on the next page.

4.5 Calculated values of ν compared with the estimated values

In the preceeding sections, the values of ν have been estimated so that agreement between the measured results and the calculated results could be obtained. In this section, these values of ν are compared with the values calculated from the formulae given in [78.1]. The values of ν from the preceeding sections are denoted US and the calculated values are denoted CA.

According to [78.1], the following expression can be used to calculate ν when the beam has stirrups as web reinforcement. The unit of f_c is MPa.

$$\nu = 0.8 - \frac{f_c}{200} \qquad (8)$$

As can be seen from table 4.5.1, the values of ν from the tests by P. Regan and M.H. Khan are somewhat smaller than the values calculated. This may be due to the fact that the bending points in these tests are not placed symmetrically about the vertical plane through the beam axis.

BEAM	f_c	f_y	f_{ys}	d	φ	ν	V	V_u	NOTES
	MPa	MPa	MPa	mm	grd.		kN	kN	
A2	34.54	276	275	12.7	45°	0.55	298	280	(1)
A3	31.85	276	275	12.7	45°	0.55	277	260	(2)
A4	32.31	269	275	9.5	45°	0.55	284	280	(2)
A5	35.38	276	275	12.7	30°	0.55	289	264	(3)
A6	30.54	276	275	12.7	60°	0.55	298	284	(4)
A8	27.85	276	275	12.7	45°	0.60	286	280	(2)
A10	34.54	276	275	12.7	45°	0.55	313	282	(3)
A13	30.08	346	275	12.7	45°	0.55	308	300	(2)
A14	32.62	346	275	12.7	45°	0.55	287	280	(2)
A15	31.77	434	275	12.7	45°	0.55	336	308	(2)
A17	24.85	640	275	12.0	45°	0.65	343	338	(2)
A18	26.85	620	275	8.0	45°	0.70	391	398	(5)
K1	24.15	427	-	15.9	26.5°	0.70	265	300	(6)
K2	27.62	276	-	12.7	45°	0.65	302	280	(2)
K4	31.54	276	-	12.7	45°	0.55	198	178	(3)

Notes: The critical yield line runs from the edge of the loading plate to

1. the third bending point.
2. the second bending point
3. the third stirrup.
4. the second stirrup.
5. the fourth stirrup.
6. the edge of the bearing plate.

Table 4.4.1 Analysis of 15 Tests by Regan and Khan

BEAM	US	CA	±	BEAM	US	CA	±
T5	0.60	0.63	-	A2	0.55	0.63	+
T12	0.60	0.63	-	A3	0.55	0.64	+
T16	0.60	0.63	-	A4	0.55	0.64	+
T13	0.70	0.64	+	A5	0.55	0.62	+
T14	0.70	0.64	+	A6	0.55	0.65	+
TA5	0.75	0.71	-	A8	0.60	0.66	+
TA17	0.75	0.67	+	A10	0.55	0.63	+
BI-1	0.66	0.69	-	A13	0.55	0.65	+
BI-2	0.55	0.68	-	A14	0.55	0.64	+
BI-3	0.64	0.68	-	A15	0.55	0.64	+
BI-4	0.65	0.68	-	A17	0.65	0.68	+
BI-5	0.72	0.70	-	A18	0.70	0.67	+
BI-6	0.74	0.68	-	K1	0.70	0.68	-
BI-7	0.84	0.68	-	K2	0.65	0.66	-
BI-9	0.68	0.68	-	K3	0.55	0.64	-
BII-11	0.87	0.68	-				

+ Stirrups and bent-up bars
- Only bent-up bars

Table 4.5.1 Estimated and Calculated Values of ν

5. CONCLUSION

It appears that the theory of plasticity provides a model which gives a reasonably good discription of the shear-strength of a reinforced concrete beam with bent-up bars as shear-reinforcement. The calculated values of the shear-strength are in good agreement with the measured ones.

The use of only bent-up bars is not advisable because of the risk of the concrete being crushed at the bending point, but a combination of stirrups and bent-up bars may be used with good results.

6. NOTATIONS

a	Length of the shear span
A	Area of the longitudinal reinforcement
A_s	Area of one cross-section of the stirrups
b	Web width
C	Compression stringer force
f_c	Uniaxial compression strength of the concrete
f_c^*	Effective strength of the longitudinal reinforcement
f_y	Yield stress of the longitudinal reinforcement
f_{ys}	Yield stress of the stirrups
h	Effective shear depth
n	Number of stirrup cross-sections cut by a yield line
s	Distance between bending points
T	Tensile stringer force
v	Relative displacement in a yield line
V	Calculated failure load
V_u	Measured failure load
x_1	Distance between the edge of the loading plate and first bending point
α	Angle between vertical and displacement vector
α_o	Optimal value of α
β	Angle between vertical and the yield line
Γ	Reduced degree of longitudinal reinforcement
ξ	Ratio between the area of the bent-up bars cut by a yield line and A
λ	a/h
ν	The web effectiveness factor
τ	Uniformly distributed shear stress
$(\frac{\tau}{f_c})_E$	Experimental shear strength
φ	Inclination of a bent-up bar
ψ	Mechanical degree of shear reinforcement
ψ_o	The value of ψ for which the yield line runs between the edges of the loading plate and the bearing plate
ϕ	Mechanical degree of longitudinal reinforcement

7. REFERENCES

[57.1] K.W. Johansen: "Critical Remarks on the Effect of Bent-up Bars and Stirrups in Reinforced Concrete Beams".
5th IABSE Congress, Lisbon 1956, Final Report, p. 507-512.

[63.1] F. Leonhardt and R. Walter: "Schubversuche an Plattenbalken mit unterschiedlicher Schubbewehrung".
Deutscher Ausschuss für Stahlbeton, Heft 156, Berlin 1963.

[67.1] K. Özden: "An Experimental Investigation on the Shear Strength of Reinforced Concrete Beams".
Technical University of Istanbul, 1967.

[71.1] K. Leksukhum and R.B. Smith: "Comparative Study of Bent-up Bars with other Forms of Secondary Reinforcement in Beams".
ACI-journal, Proceedings V.68, No. 1, Ja. 1971, p. 32-35.

[71.2] P. Regan: "Shear in Reinforced Concrete, an Experimental Study".
Imperial College of Science and Technology, Department of Civil Engineering 1971, p. 63-92.

[72.1] Hans Chr. Sørensen: "Efficiency of Bent-up Bars as Shear Reinforcement".
Bygningsstatiske Meddelelser, vol. 43, p. 105-122, 1972.

[75.1] M.P. Nielsen and M.W. Bræstrup: "Plastic Shear Strength of Reinforced Concrete Beams".
Bygningsstatiske Meddelelser, vol. 46, no. 3, 1975, p. 61-99.

[78.1] Nielsen, M.P., Bræstrup, M.W., Jensen, B.C. and Bach, F.: "Concrete Plasticity".
Danish Society for Structural Engineering and Science, Special Publication, October 1978.

[78.2] Nielsen, M.P., Bræstrup, M.W. and Bach, F.: "Rational Analysis of Shear in Reinforced Concrete Beams".
IABSE proceedings, P - 15/78, May 1978.

[78.3] Pedersen, C., Jensen, J.F., Nielsen, M.P. and Bach, F.: "Opbøjet længdearmering som forskydningsarmering" (Bent-up Bars as Shear Reinforcement) (In Danish).
Structural Research Laboratory, Technical University of Denmark, Report No. R100, November 1978.

II

The Stringer Method Applied to Discs with Holes

La méthode des „stringers" appliquée aux parois avec des ouvertures

Anwendung der Stringermethode auf gelochte Scheiben

J.C. KAERN
PhD Student
Technical University of Denmark
Lyngby, Denmark

SUMMARY
In this paper a simple method — the stringer method — is discussed for constructing lower-bound solutions for reinforced concrete discs with holes. In the method normal stresses are concentrated in lines, the stringers, forming an orthogonal net. The rectangular areas between the stringers are assumed to carry pure shear only. The use of the method is described by simple examples. Further, the problem of optimizing the statical and geometrical variables is dealt with.

RESUME
Des valeurs inférieures pour la charge ultime de parois avec des ouvertures sont obtenues à l'aide d'une méthode simple. La paroi est divisée par un réseau orthogonal de „stringers". L'état de contrainte dans les éléments rectangulaires limités par les „stringers" est supposé un état de cisaillement pur. Les contraintes normales par rapport aux axes du réseau orthogonal sont concentrées dans les „stringers". L'application de la méthode est décrite à l'aide d'exemples simples. Le problème du choix optimal des variables statiques et géométriques est discuté.

ZUSAMMENFASSUNG
Untere Grenzwerte für die Traglast von gelochten Scheiben werden mit einer einfachen Methode ermittelt. Die Scheibe wird mit einem rechtwinkligen Netz von Stringern in rechteckige Elemente unterteilt. Es wird angenommen, in den rechteckigen Elementen herrsche ein Zustand reinen Schubes, und die Normalspannungen bezüglich der Netzrichtungen werden als in den Stringern konzentriert wirkende Kräfte zusammengefasst. Die Anwendung der Methode wird mit einfachen Beispielen erläutert, und das Problem der optimalen Wahl der statischen und geometrischen Variablen wird erörtert.

1. INTRODUCTION

In aeroelasticity it has for a long time been customary to apply the stringer method for the calculation of thin sheets reinforced with stringers in the elastic region. Within reinforced concrete design in the plastic region, the stringer method was applied to cylindrical shells by Lundgren [1] and to discs by Nielsen [2] [3].

In this paper it is demonstrated how the method provides a useful tool for treating discs with holes. In addition, the method is concisely described in general terms since it still seems to be rather unknown within the concrete field.

2. CALCULATION OF DISCS

Reinforced concrete discs are still often designed by calculating the stresses according to the elastic theory. However, the reinforcement is generally designed according to one or another plastic theory. Such a procedure has often great disadvantages since the elastic stress field may have large stress peaks for which a correct reinforcement is unpractical. Therefore, even when elastic design is used, the stresses are often only covered by reinforcement in some average manner.

Some simple and often-met design problems are relatively well dealt with by experiments so that empirical formulas can be developed. For discs with holes, such formulas have been developed by Kong [4].

A more rational method of design is furnished by the theory of plasticity.

If the lower bound method is applied, one needs a statically admissible stress field. The necessary reinforcement can then be determined by standard formulas. A number of statically admissible solutions for discs without holes have been given in [2] and [3]. Most of them are constructed by combining homogeneous stress fields in triangular elements. This type of stress field could also be used in discs with holes, but solutions for practical purposes have not yet been developed.

In the following it is shown how the stringer method can be applied to discs with holes.

3. THE STRINGER METHOD

The basic idea of the stringer method is that the normal stresses are imagined carried by stringers, i.e. lines along which concentrated tensile or compressive forces are located. The stringers are supposed to form an orthogonal net. The rectangular elements between the stringers are supposed to be subjected to constant pure shear. Therefore, the stringer forces vary linearly between the net points.

If necessary, the external forces of course have to be replaced by an equivalent set of concentrated forces in the net points and constant shear stresses along the boundaries of the rectangular elements.

The idealized system will normally be statically indeterminate. If the shear stresses in the rectangular elements are considered to be the unknowns, it means that a number of shear stresses can be chosen arbitrarily. When the statically indeterminate shear stresses have been chosen, the other ones can be determined by equilibrium equations. Knowing the shear stresses, the stringer forces can finally be determined.

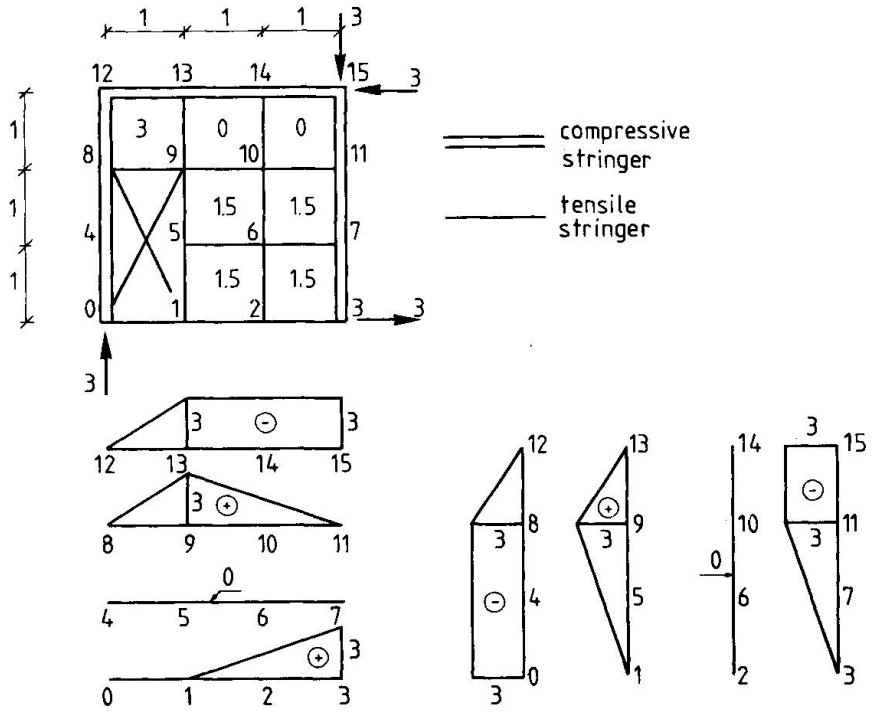

Fig. 1.

A simple example as shown in Figure 1 illustrates this procedure. This figure shows a disc with a hole 0,1,9,8. The disc may be imagined to be half of a deep beam with the depth equal to 3 units and the span equal to 6 units. The thickness is assumed to be 1 unit. In the middle section, the moment is supposed to be carried by concentrated forces at the top and bottom. The external load is a concentrated force of 3 units in the middle point at the top side. The disc has been divided into stringers as shown in the figure. Vertical projection shows that the shear stress in the element 8,9,12,13 is 3. Choosing the shear stress in 9,10,13, 14 to be zero and the shear stress in 5,6,9,10 to be 1,5, vertical projection shows that the shear stress in 1,2,5,6 is 1,5. Horizontal projection shows that the shear stress in 10,11,14,15 is 0, that the shear stress is 1,5 in 6,7,10,11 and that the shear stress is 1,5 in 2,3,6,7. Vertical projection through the 3 elements to the right is automatically satisfied. It is seen that in this case, there are 2 statically indeterminate shear stresses. The stringer forces can now easily be determined. The result is shown in the figure.

The stringer method can be explained in general terms by using Airy's stress function. The function for the force system in the stringer theory is a number of hyperbolic paraboloids, one for each rectangular element.

The stresses in rectangular coordinates x,y is generally

$$\sigma_x = \frac{\partial^2 \psi}{\partial y^2} \tag{1}$$

$$\sigma_y = \frac{\partial^2 \psi}{\partial x^2} \tag{2}$$

$$\tau_{xy} = -\frac{\partial^2 \psi}{\partial x \partial y} \tag{3}$$

σ_x and σ_y being normal stresses (positive as tensile stresses), τ_{xy} the shear stress and Ψ the Airy stress function, it is seen that the hyperbolic paraboloids give constant shear stresses in the rectangular elements since $\partial^2\Psi/\partial x\partial y$ will be constant. The jumps in the derivatives $\partial\Psi/\partial x$ and $\partial\Psi/\partial y$ in the net points determine

the concentrated stringer forces.

From the general theory of plane stress, it is known that the values of Ψ and of the derivatives $\partial\Psi/\partial x$ and $\partial\Psi/\partial y$ are determined along the boundary. Using the properties of the stress function, it is easily shown that the number, N , of statically indeterminate shear stresses is

$$N = m - h - (2s - y) + (r - 3) \tag{4}$$

where

- m is the number of net points incl. the number of net points in holes.
- h is the number of rectangular elements where the shear stress is zero.
- s is the number of stringers running from boundary to boundary (incl. boundaries along holes).
- y is the number of external stringers, i.e. stringers having a boundary on one side of the stringer along the whole stringer.
- r is the number of reactions.

In the case shown in Figure 1, we have m = 16, h = 2, s = 8, y = 4 and r = 3, giving N = 2, as already found.

In the more complicated example shown in Figure 2, we have m = 86, h = 9, s = 23, y = 4 and r = 4, giving N = 36.

The validity of formula (4) is demonstrated by the following arguments: The stress function Ψ is determined by m parameters. N is found as m minus the number of requirements to the shear stress in holes and the number of requirements to the stringer forces at the boundaries. For an internal stringer, there are two boundary conditions since the stringer force is determined as differences between first derivatives of the stress function. For an external stringer with a boundary on one side along the whole stringer, the stringer force is not determined in an analogous way, but a projection equation can be formulated giving one requirement. The last term in (4) is the number of external statical indeterminate parameters.

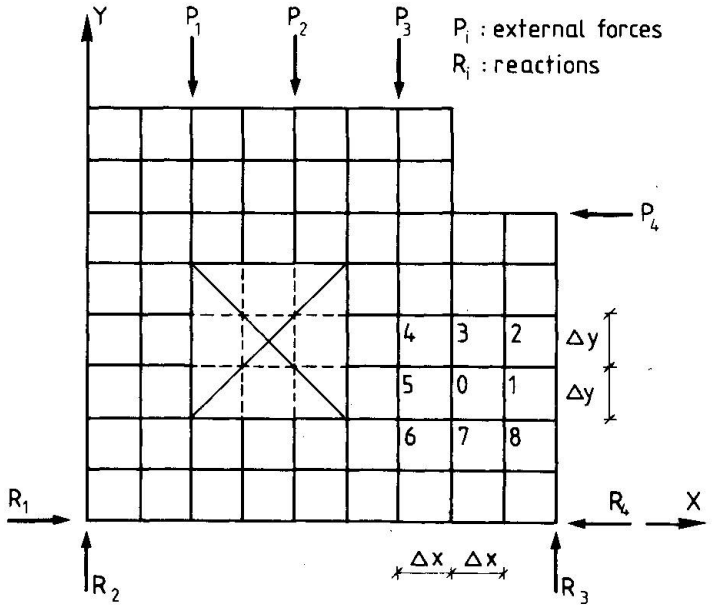

Fig. 2.

If the number of net points is large, the force system in the stringer method can be used as an approximation of a continuous stress field. If the stringer forces are distributed uniformly along Δx and Δy, Δx and Δy being the distance between the net points in the x-direction and the y-direction resp., we find at the point 0 in Figure 2:

$$\sigma_x = \frac{\Psi_3 - 2\Psi_0 + \Psi_7}{(\Delta y)^2} \tag{5}$$

$$\sigma_y = \frac{\Psi_1 - 2\Psi_0 + \Psi_5}{(\Delta x)^2} \tag{6}$$

$$\tau_{xy} = \frac{(\Psi_4 + \Psi_8) - (\Psi_2 + \Psi_6)}{4\Delta x\, \Delta y} \tag{7}$$

Note that these expressions are identical to the usually applied difference approximations.

In order to get a situation at the boundary equivalent to the situation at interiour points, the boundary stringers may be placed at a distance $\Delta x/2$ and $\Delta y/2$ resp. from the real boundary.

4. OPTIMIZED STRINGER SYSTEMS

The stringer is a practical tool which can offer a quick answer to the question of how to reinforce a disc for given external loads. Therefore, the method is especially well suited for hand calculations giving simple solutions to a reinforcement problem.

In more refined calculations, one may wish to find the optimum value of the statically indeterminate quantities, i.e. the values giving the smallest amount of reinforcement. One may even wish to find the optimum lay-out of a stringer system.

As an example, consider a rectangular hole in a zone with pure shear. The question how to reinforce the disc near the hole can be answered by considering a stringer system as shown in Figure 3.

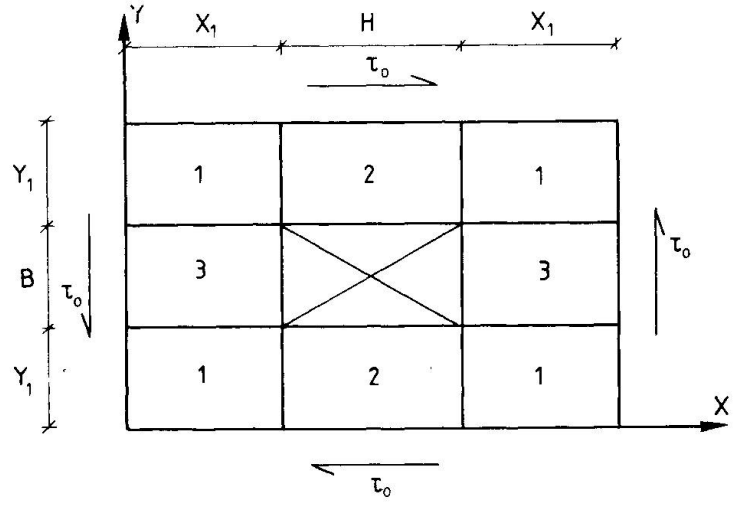

Fig. 3.

If the shear stress outside the stringer system is τ_0 and if the geometry of the stringer system is, for instance, laid down as shown in the figure, the shear stresses and the stringer forces can be calculated as explained above. Here, the

reinforcement is chosen as a homogeous mesh and a constant reinforcement area along the whole length of the stringer, but different in vertical and horizontal directions. The necessary reinforcement may then be determined by the formulas given in [2] and [3]. Because of symmetry, the shear stresses in the rectangular element having the same number in the figure are equal. The shear stresses are then statically determinate if x_1 and y_1 are known. The total reinforcement volume can then be determined as a function of x_1 and y_1 and then minimized with respect to these quantities.

The result of such an optimization is shown in Figure 4.

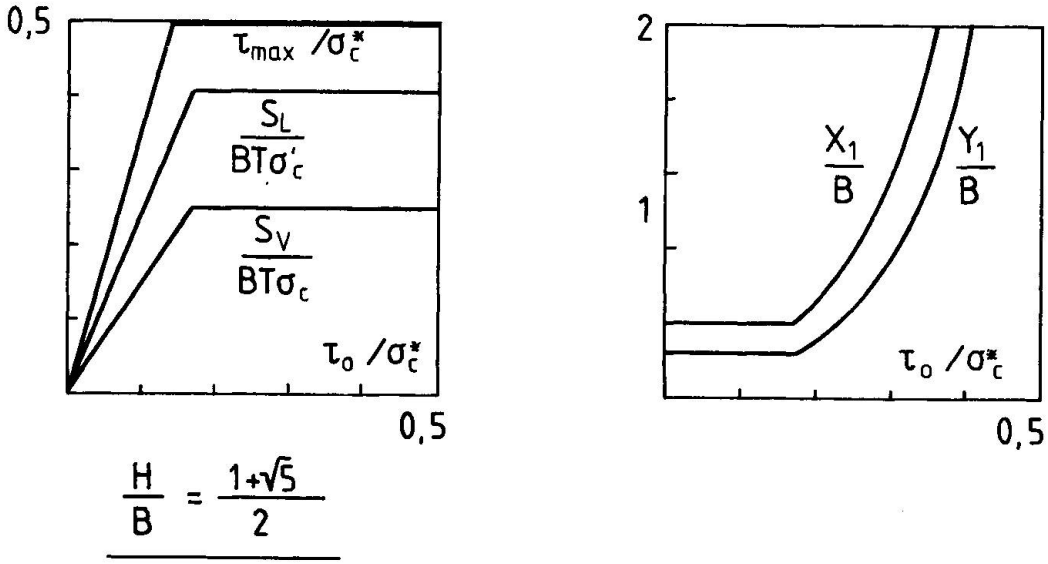

Fig. 4.

In the figure, σ_c^* is the effective concrete compression strength of the concrete, S_L is the largest value of the stringer force in vertical stringers and S_V the largest stringer force in horizontal stringers. The optimal value of the geometrical parameters x_1 and y_1 tends to infinity if τ_0 approaches $\sigma_c^*/2$, which is the largest shear stress which can be carried by concrete in plane stress conditions.

Similar optimizations can be carried out in other cases. Some results have been described in [6].

If the stringer system has such a fine mesh that a continuous stress field can be modelled, the optimization can be formulated as a linear programming problem, provided that the yield condition for the reinforced material is linearized. Such a procedure has been developed in [5], using, however, a difference approximation for the stress components as a function of the net point values of the Airy stress function. Therefore, these net point values can be used as optimization variables. However, an optimization could just as well take place by means of the stringer method, using the shear stresses as variables, whereby the boundary conditions could perhaps be handled in an easier way than in the difference method. This, however, has yet to be demonstrated.

REFERENCES

1. LUNDGREN, H.: Cylindrical Shells. The Danish Technical Press. The Institute of Civil Engineers, Copenhagen 1949.

2. NIELSEN, M.P.: Om jernbetonskivers styrke. Polyteknisk forlag, København 1969.

3. NIELSEN, M.P.: On the Strength of Reinforced Concrete Discs. Acta Polytechnica Scandinavica, Copenhagen 1971.

4. KONG, F.K.: Structural Idealization for Deep Beams with Web Openings Further Evidence. Magazine of Concrete Research, Vol. 30, No. 103, pp. 89 - 94, June 1978.

5. BRYDER, K.: Optimeringsmetoder for 2-dimensionale legemer af ideal plastiske materialer. (Optimization Methods for 2-Dimensional Bodies of Perfectly Plastic Materials). Ph.D. thesis, Structural Research Laboratory, Technical University of Denmark, Lyngby, September 1978.

6. KÆRN, J.C.: Optimering af armering omkring huller i skiver. (Optimization of Reinforcement around holes), Structural Research Laboratory, Technical University of Denmark, Internal Report (in press), Lyngby 1979.

Leere Seite
Blank page
Page vide

II

Plastic Analysis of Reinforced Concrete Panels in Frames

Analyse plastique d'éléments d'un cadre, composés de panneaux en béton armé

Plastische Berechnung von durch Rahmen umschlossenen Wandelementen aus Stahlbeton

P.A.C. SIMS
Senior Scientific Officer
Building Research Establishment
Watford, England

SUMMARY

Plastic analysis of reinforced concrete panels in frames is considered by assuming that recently identified collapse modes for unreinforced panels are also applicable to reinforced panels.
Two of these modes, shear mode S and shear-rotation mode SR, are shown to be valid by obtaining upper and lower bound solutions. The direct compression mode DC is shown to be valid only for a very restrictive range of panels with considerable differences existing between the upper and lower bound solutions.

RESUME

L'analyse plastique des panneaux en béton armé, éléments d'un cadre, est faite en supposant que les modes de rupture récemment identifiés pour les panneaux en béton sans armature sont également applicables aux panneaux en béton armé. La validité de deux de ces modes — le mode de cisaillement S et le mode de cisaillement-rotation SR — est démontrée à l'aide des solutions cinématiques et statiques correspondantes. Le mode de compression-directe DC n'est valable que pour une série très limitée de panneaux, avec des différences considérables entre les valeurs inférieures et supérieures de la charge ultime.

ZUSAMMENFASSUNG

Von der Annahme ausgehend, dass die vor kurzem gefundenen Kollapszustände für unbewehrte Wandelemente auch für den Fall bewehrter Elemente anwendbar sind, werden Wandelemente aus Stahlbeton, die durch Rahmen umschlossen sind, mit Hilfe der Plastizitätstheorie untersucht. Die Gültigkeit von zweien dieser Zustände, kurz als Typ S (Schiebung) beziehungsweise SR (Schiebung-Rotation) bezeichnet, wird mit Hilfe kinematischer und statischer Lösungen nachgewiesen. Wie gezeigt wird, tritt der dritte betrachtete Zustand, Typ DC (direkte Abstützung), nur für eine sehr beschränkte Auswahl von Wandelementen auf. Hier bestehen erhebliche Unterschiede zwischen den erhaltenen oberen und unteren Grenzwerten für die Traglast.

1. INTRODUCTION

Where wall panels are built in-line with frameworks, the resistance to in-plane horizontal loads increases considerably due to composite action between the frame and the panel. From the few known full-scale tests to destruction and many more model tests on unreinforced panels at the Building Research Station[1],[2], distinct collapse modes could be identified and idealised, Fig 1.

A theory to distinguish between these modes and their associated collapse loads for unreinforced panels has only recently been published by Wood [3], based on plasticity theory, which predicted these modes in their correct order of increasing relative frame/panel strength.

The small number of tests relating to reinforced panels has meant that the different collapse modes have not necessarily been observed and thus this paper extends Wood's approach by assuming that the idealised unreinforced panel modes can be applied to reinforced panels.

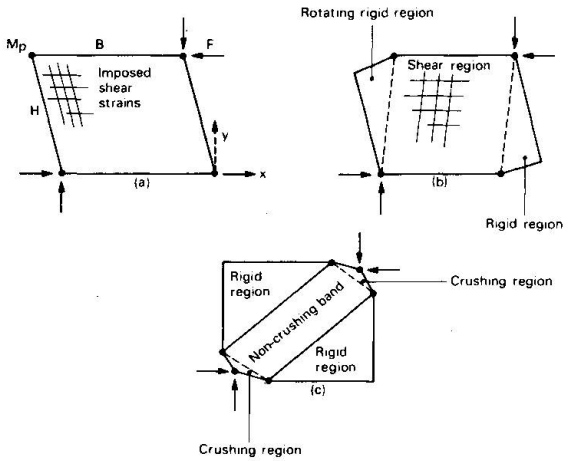

Fig 1 Idealised plastic failure modes (a) Shear mode *S*; (b) Shear rotation mode *SR*; (c) Corner crushing diagonal mode *DC*

2. PLASTICITY THEORY OF REINFORCED PANELS SUBJECT TO IN-PLANE HORIZONTAL LOADS

2.1 Yield criterion

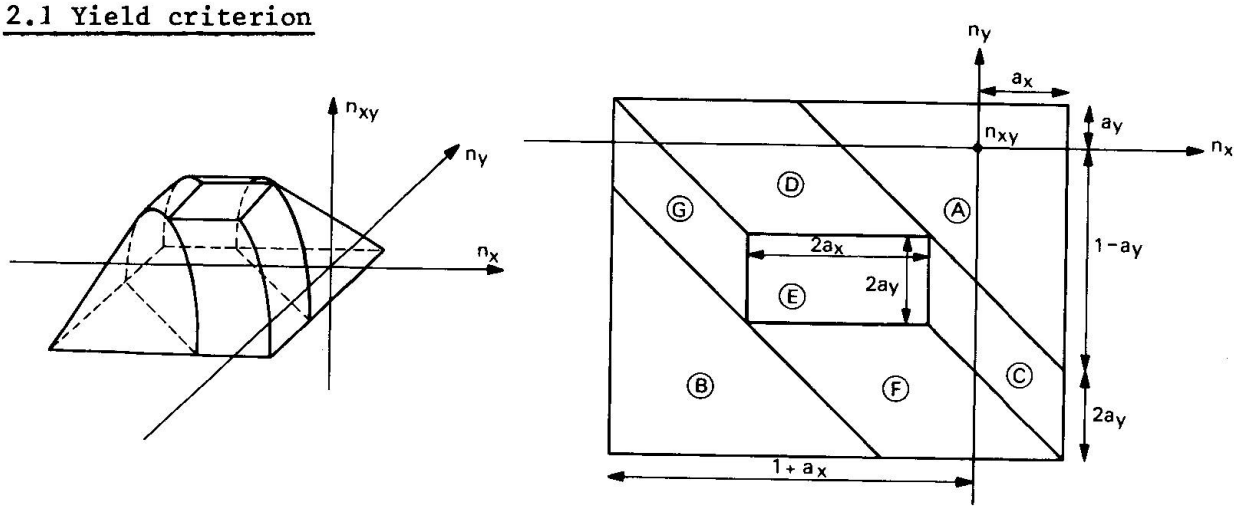

Fig 2 Yield criterion for orthogonally reinforced panel elements

The yield criterion assumed is due to Nielsen [4], shown in Fig 2, and outlined by Morley [5] and Marti [6]. It should be noticed that certain regions of the criterion introduce indeterminacy into the calculation of stress components corresponding to assumed strain rates via the flow rule. For upper bound solutions these components are usually accompanied by zero components of the strain-rate but for lower bound solutions, guided by the upper bound stress fields, this indeterminacy causes non-unique stress fields which satisfy equilibrium.

2.2 Composite shear mode *S*

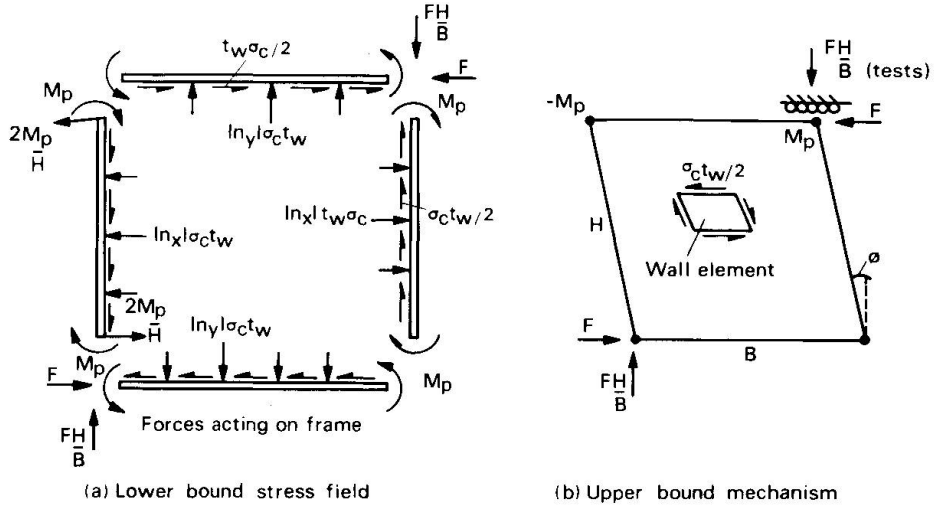

(a) Lower bound stress field (b) Upper bound mechanism

Fig 3
Shear mode *S*

All modes will be examined with equal plastic moments in the beams and columns. The assumed mechanism (Fig 3b) has a dissipation of energy in the frame of $4M_p\phi$ provided that the joints are rigid. For small displacements a rectangular frame would not require any extension of the panel only pure shear. Reference to the yield criterion, Fig 2, shows that the stress point associated with a strain-rate $(0, 0, -\phi)$ is

$$\left(-(\tfrac{1}{2}+a_x) \leqslant n_x \leqslant -(\tfrac{1}{2}-a_x),\ -(\tfrac{1}{2}+a_y) \leqslant n_y \leqslant -(\tfrac{1}{2}-a_y);\ n_{xy} = \pm\tfrac{1}{2}\right)$$

The energy dissipated in the panel is thus $BH\phi t_w\sigma_c/2$ and the work equation leads to an upper bound collapse load of

$$F = 4M_p/H + \tfrac{1}{2}\sigma_c t_w B \qquad (1)$$

The lower bound stress field is shown in Fig 3a where n_x and n_y are constrained to lie within the ranges

$$-(\tfrac{1}{2}+a_x) \leqslant n_x \leqslant -(\tfrac{1}{2}-a_x);\ -(\tfrac{1}{2}+a_y) \leqslant n_y \leqslant -(\tfrac{1}{2}-a_y)$$

By considering the equilibrium of the beams and columns it can be shown that

$$F = 4M_p/H + \tfrac{1}{2}\sigma_c t_w B \quad \text{ie equation (1)}$$

Thus equation (1) is an exact solution provided that M_p is not exceeded anywhere in any of the beams or columns. Consideration of the bending moment in the top beam shows that the minimum permissible plastic moment is reached when the shear force at the left hand end is zero, ie $2M_p/B - \tfrac{1}{2}|n_y|\sigma_c t_w B = 0 \qquad (2)$

Introducing Wood's [3] definition of f and m,

$$f = F/(4M_p/H + \tfrac{1}{2}\sigma_c t_w B);\quad M = 8M_p/\sigma_c t_w B^2$$

then $f = 1$ providing for the beam $m \geqslant 2|n_y|$

Similarly, examination of the column gives the condition as $m \geqslant 2|n_x|H^2/B^2$

Thus if either of these conditions are violated, negative hinges could appear in the beam and/or columns marking the termination of mode *S*. Hence it is the accompanying direct stresses which are responsible for the change from the pure shear mode.

2.3 Shear rotation mode *SR*

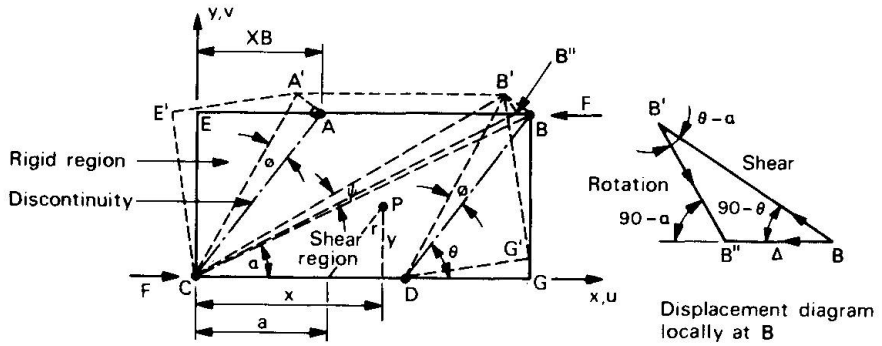

Fig 4 Mode *SR* upper bound

The negative moment hinge now appears at a point *XB* from the end *E* of the beam (Fig 4). The inclined discontinuities *CA* and *DB* separate the end rigid regions from the shearing region *ABCD*. Since *CEA* remains rigid it rotates to *CE'A'* through an angle ϕ and the original rectangle is distorted to *CE'A'B'G'D*. However imposition of the boundary conditions requires a rigid body rotation of the whole panel through an angle ψ about *C*, so as to bring *B'* to *B''*. As $\psi \ll \alpha$, *B'B''* is virtually perpendicular to *CB'*, Fig 5, from which it can be shown that

$$\phi = \Delta \sin\theta \cos\alpha / (H \sin(\theta - \alpha)) \qquad (3)$$

A further consequence of the discontinuities *CA* and *DB* is that there is expansion of the shear region in the y direction but none in the x direction.

From the displacement of a point *P*, Fig 4, the strain-rate in the shearing region can be deduced as

$$\varepsilon_x = 0;\ \varepsilon_y = \phi \cot\theta;\ \varepsilon_{xy} = -\phi \qquad (4)$$

Region *D* of the yield criterion, Fig 2, is able to support these strain-rate components and it can be shown that the stress point corresponding to (4) is given by

$$n_y = -(1 - 2a_y - \cos\theta)/2;\ n_{xy} = -(\sin\theta)/2$$

with n_x lying within the range

$$-(1 + 2a_x + \cos\theta)/2 \leq n_x \leq -(1 - 2a_x + \cos\theta)/2$$

Since the stresses and strain-rates are constant over an area $BH(1 - X)$ the dissipation of energy in the panel can be expressed as

$$D_w = \tfrac{1}{2}\sigma_c t_w \phi BH(1 - X)\left[\sin\theta - (1 - 2a_y - \cos\theta)\cot\theta\right] \qquad (5)$$

Adding the frame dissipation, again $4M_p\phi$; equating to the external work $F\Delta$, and substituting for ϕ from (3), leads to

$$f = \left[Bm/H(1 - X) + \sqrt{1 + (BX/H)^2} - (1 - 2a_y)BX/H\right]/(1 + mB/H) \qquad (6)$$

This equation is minimised numerically for X to obtain the best upper bound.

For the lower bound a stress point lying within region *D* of the yield criterion will be assumed. Such a point requires two parameters $n_x = -C_x$ and $n_y = -C_y$ since the shear component will be determined from the yield criterion's equations.

To ensure that the point remains within D, C_x and C_y must satisfy

$$C_y \leqslant (\tfrac{1}{2} - a_y) \text{ and } 1 - a_x - a_y \leqslant C_x + C_y \leqslant 1 + a_x - a_y \qquad (7)$$

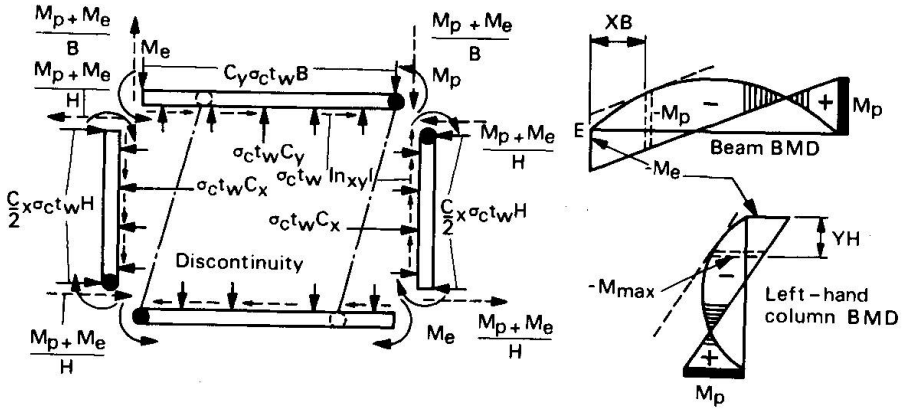

Fig 5 Mode *SR* lower bound

With this stress field the forces acting on the frame are as shown in Fig 5. Even though the discontinuity would permit a change in the stress component parallel to the discontinuity in the triangular regions, a continuous stress field is assumed throughout. A negative plastic moment is enforced in the beams at the ends of the discontinuities, resulting in the moment at the non-loaded beam-column junction no longer being plastic. For the solution, in addition to the three equilibrium conditions for each beam and column, there are two conditions relating to the position of the minimum moment in the beam. Firstly that this position has zero shear and secondly that this is a plastic moment. Solving these results in

$$X = 1 - \sqrt{m/2C_y} \qquad (8) \qquad\qquad M_e/M_p = 1 - 4C_y X^2/m \qquad (9)$$

The columns must be checked to ensure that overstressing does not result and a section distance YH from the bottom of the right hand column is examined for minimum moment and zero shear. This results in

$$Y = \tfrac{1}{2}\left\{1 + (B^2/H^2)(C_y/C_x)(X^2 - m/2C_y)\right\} \qquad (10)$$

$$M_{max}/M_p = 1 - 4C_x (1 - Y)^2 H^2/mB^2 \qquad (11)$$

Finally the expression for f is obtained as

$$f = 2\left[C_y(1 - 2X)B/H + \sqrt{(1 - a_y - C_y)(a_y + C_y)}\right] / (1 + mB/H) \qquad (12)$$

f is maximised numerically for trial C_x and C_y values within the range defined by equation (7) using the following strategy:

- (a) X must be in the range $0 \leqslant X \leqslant 1$.
- (b) M_e/M_p from (9) must be within the range - 1 to + 1.
- (c) If Y from (10) is positive then $|M_{max}/M_p| \leqslant 1$.
- (d) If Y is negative then the value returned for M_{max}/M_p is ignored.
- (e) If either M_e/M_p or M_{max}/M_p exceeds unity then a valid lower bound can still be obtained providing f is divided by the largest of these values.

From equations (10) and (11) C_x merely affects the degree and position of the

minimum moment in the columns. For a given C_y, any value of C_x is acceptable which satisfies (7) and conditions (c) and (d) above without generating (e) if possible. This is usually achieved by selecting the lower end value of the range.

Specimen results of the upper and lower bound solutions are shown in Table 1.

B/H	m	a_x	a_y	f_{LB}	f_{UB}
1	0.2	0.1	0.1	0.8333	0.9060
1	0.5	0.1	0.1	0.9766	0.9861
1	0.3	0.05	0.05	0.8763	0.9251
2	0.25	0.1	0.1	0.9210	0.9210
2	0.6	0.05	0.05	0.9867	0.9867

Table 1 Comparison of mode *SR* upper and lower bound solutions

2.4 Diagonal compression mode *DC*

The lower bound solution for this mode assumes that the distribution of load by the frame to the panel is such as to cause a diagonal band stressed to its maximum, leaving the remaining regions rigid and stress free. To allow for orthotropic reinforcement, a band orientated as shown in Fig 6a has been assumed allowing two parameters Y and X. However this solution, in general violates

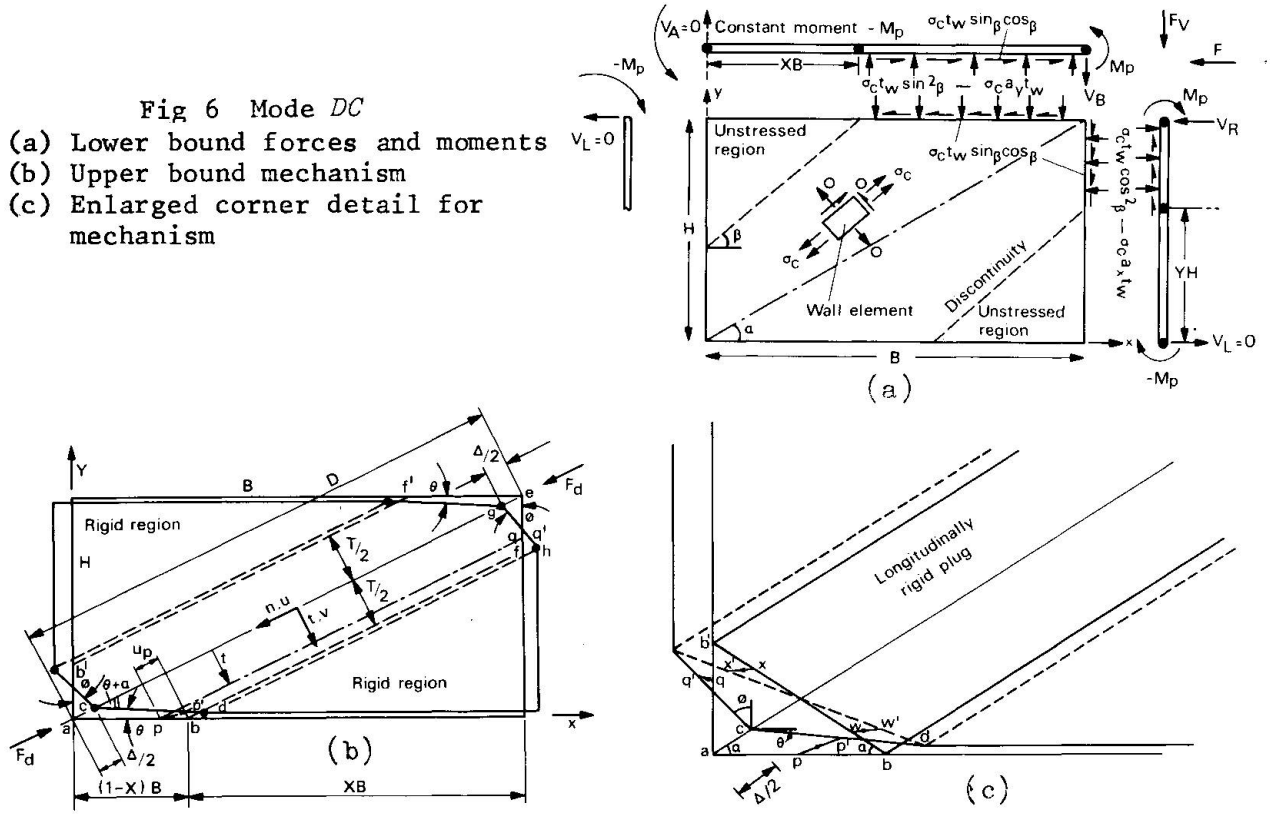

Fig 6 Mode *DC*
(a) Lower bound forces and moments
(b) Upper bound mechanism
(c) Enlarged corner detail for mechanism

global equilibrium requirements unless a band parallel to the panel diagonal is assumed resulting in a very restricted set of panel parameters for which the solution is valid. Thus a more general solution free from these restrictions, is required and is currently under investigation. Where the solution is valid X, Y and f are given by

$$X = 1 - \sqrt{m/2(\sin^2\beta - a_y)} \qquad (13); \quad Y = 1 - \sqrt{mB^2/2H^2(\cos^2\beta - a_x)} \qquad (14)$$

$$f = 2\left[(1 - Y)(\cos^2\beta - a_x)H/B + (1 - X)\sin\beta\cos\beta\right]/(1 + mB/H) \qquad (15)$$

Since the lower bound is restricted this is reflected in the upper bound mechanism, Figs 6b and 6c, which has a parallel diagonal band containing a

diagonally rigid region, so that crushing is confined to the triangular regions at opposite ends of this band. This rigid region is allowed to shear and expand transversely which is ensured by insisting that bb' and ff', Fig 6c, rotate but remain parallel. Details of this mechanism can be found in Wood's paper [3] but modification is needed since the yield criterion requires the strain-rate components to be in the direction of the reinforcement bars and not parallel and perpendicular to the panel diagonal. Performing this transformation, and determining the corresponding stress points and resulting energy dissipation, in a similar manner to that for mode *SR*, results in

$$f = \left[1 + Bm/H(1 - X) - 2(1 - a_x - a_y)BX/H(1 + (B/H)^2)\right]/(1 + mB/H) \qquad (16)$$

The minimum is found by differentiation and occurs when

$$X = 1 - \sqrt{m(1 + B^2/H^2)/2(1 - a_x - a_y)} \qquad (17)$$

For solution purposes these equations are evaluated separately to ensure that X remains in the range $0<X<1$.

3. COMPARISON OF THE UPPER AND LOWER BOUND SOLUTIONS

Plotted curves of the various solutions proved to be overlapping and confusing, as indicated by the lower bound solutions for square panels having isotropic reinforcement, Fig 7. The trend of solutions has thus been indicated by tabulating the best solutions for $a_x = 0.1$, $a_y = 0.1$, with a code to indicate which mode applies, Table 2. Unlike the unreinforced case, there are no analytical expressions valid throughout the range of m, nor are there any analytically exact solutions. For non-square panels mode *SR* solutions are numerically exact to ten decimal places, providing that the lower bound has not been modified due to column overstress. For square panels with isotropic reinforcement, mode *SR* lower bound is numerically equal to mode *DC* upper bound until, again, column overstress causes a rapid fall off in the *SR* lower bound, Fig 7, which is then superseded by the mode *DC* lower bound. This result is due to the symmetry of this case since a plastic hinge would be expected to form in the column also; a fact confirmed by noting that the best lower bound for *SR* occurs when the column overstress factor is unity.

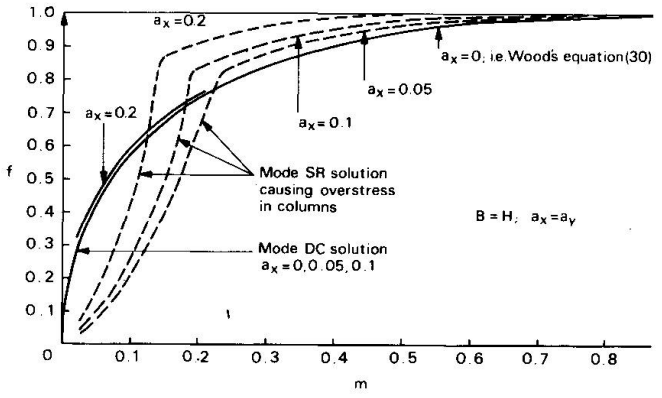

Fig 7 Lower bound solutions for square panels with isotropic reinforcement

m	Best lower bound for f		Best upper bound for f	
	$B/H = 1$	$B/H = 2$	$B/H = 1$	$B/H = 2$
0.8	1.0 *S*	1.0 *S*	1.0 *S*	1.0 *S*
0.6	0.9910 *SR*	0.9944 *SR*	0.9910 *DC*	0.9944 *SR*
0.4	0.9510 *SR*	0.9693 *SR*	0.9510 *DC*	0.9693 *SR*
0.25	0.8755 *SR*	0.9210 *SR*	0.8755 *DC*	0.9210 *SR*
0.2	0.8333 *SR*	0.8938 *SR*	0.8333 *DC*	0.8938 *SR*
0.15	0.6778 *DC*	0.8566 *SR*	0.7764 *DC*	0.8574 *SR*
0.1	0.5785 *DC*	0.7940 *SR*	0.6961 *DC*	0.8069 *SR*
0.05	0.4286 *DC*	0.3684 *SR*	0.5714 *DC*	0.7331 *SR*

Table 2 Example of the best upper and lower bound solutions

For rectangular panels and for square panels with orthotropic reinforcement, the general solution is hampered by the restrictions placed on the validity of the mode *DC* lower bound, but even where this solution is valid, eg Fig 7, there is a considerable jump between the solutions for modes *DC* and *SR*, suggesting that

there are better solutions for panels having small m values. For square panels with orthotropic reinforcement, the trend from the number of cases evaluated to date is that as well as both *SR* solutions being unequal, the equality between *SR* lower bound and *DC* upper bound has disappeared.

4. CONCLUSION

An introduction of plasticity analysis to reinforced concrete panels in frames has been achieved by assuming that the modes observed for unreinforced panels are applicable. For single panels having equally strong beams and columns analytically exact solutions for the pure shear mode *S* have been obtained for all panels; numerically exact solutions for the shear-rotation mode *SR* have been obtained for rectangular panels and for square panels having isotropic reinforcement, and a very restrictive set of conditions has been determined for which the diagonal compression mode *DC* is valid. This latter point suggests that either there are better solutions for this mode or that a more suitable mode exists.

5. NOTATION

A_x, A_y area of reinforcement in the co-ordinate directions per unit width of panel.

σ_Y magnitude of the yield stress of the reinforcement bars.

N_x, N_y, N_{xy} membrane forces per unit width of panel element.

$$n_x = \frac{N_x}{\sigma_c t_w} \quad n_y = \frac{N_y}{\sigma_c t_w} \quad n_{xy} = \frac{N_{xy}}{\sigma_c t_w} \quad a_x = \frac{A_x \sigma_Y}{\sigma_c t_w} \quad a_y = \frac{A_y \sigma_Y}{\sigma_c t_w}$$

6. ACKNOWLEDGEMENT

This paper is published by permission of the Director of the Building Research Establishment and forms part of the current research programme. The author is indebted to Dr R H Wood, formerly of the Building Research Establishment, for his invaluable help during this work.

7. REFERENCES

1 WOOD, R H. The stability of tall buildings. Proc Instn Civ Engrs, 11, Sept, (1958), 69-102

2 MAINSTONE, R J and WEEKS, G A. The influence of a bounding frame on the racking stiffnesses and strengths of brick walls. Proc 2nd Int Brick Masonry Conf, (1970), 165-171

3 WOOD, R H. Plasticity composite action and collapse design of unreinforced shear wall panels in frames. Proc Instn Civ Engrs, Part 2, 65, June, (1978), 381-411

4 NIELSEN, M P. On the strength of reinforced concrete discs. Acta Polytech Scand., Series 70, Bulletin 2, (Copenhagen), (1971)

5 MORLEY, C T. Yield criteria for elements of reinforced concrete slabs. Plasticity in Reinforced Concrete, Introductory Report, IABSE Colloquium, Zurich, (1979), 35-47

6 MARTI, P. Plastic analysis of reinforced concrete shear walls. Plasticity in Reinforced Concrete, Introductory Report, IABSE Colloquium, Zurich, (1979), 51-69

II

Plastic Analysis of Torsion and Shear in Reinforced Concrete

Analyse plastique du béton armé soumis à la torsion et au cisaillement

Plastische Berechnung für Torsion und Schub im Stahlbeton

P. MUELLER
Dr.sc.techn., dipl. Ing. ETH
Massachusetts Institute of Technology
Cambridge, Massachusetts, U.S.A.

SUMMARY
Collapse mechanisms for reinforced concrete beams in torsion, bending and shear are presented. The mechanisms complete the truss model solution to an exact plastic solution. The shear strength of deep beams and of beam regions near supports or point loads is explored.

RESUME
Des mécanismes de ruine pour des poutres en béton armé sous torsion, flexion et effort tranchant sont présentés. Ces mécanismes complètent le modèle de treillis pour constituer une solution plastique exacte. On étudie la résistance ultime à l'effort tranchant des régions d'appuis ou d'application des charges et des poutres courtes.

ZUSAMMENFASSUNG
Kollapsmechanismen für Stahlbetonbalken unter Torsion, Biegung und Querkraft werden dargestellt. Die Mechanismen vervollständigen die Fachwerkmodellösung zu einer plastizitätstheoretisch exakten Lösung. Die Schubtragfähigkeit von Balken in Lasteinleitungsbereichen und von wandartigen Trägern wird untersucht.

1. INTRODUCTION AND ASSUMPTIONS

In recent years the theory of plasticity has considerably contributed to both the understanding of shear transfer and the determination of the shear strength in reinforced (prestressed or mild) concrete [1]. This paper reports on some results of two studies [2,3] contributing to a rational and consistent plastic theory for reinforced concrete beams, deep beams and shear walls. First collapse mechanisms for beams in torsion, bending and shear are presented. Second some plane stress problems related with the shear strength of beams near supports and of deep beams are treated.

It is assumed that webs and flanges of beams and walls can be modeled as elastic-perfectly-plastic membranes governed by the yield criterion derived from the no tensile strength, square yield criterion for concrete (Figs. 1 and 2). The states of stress and motion are described in terms of membrane forces per unit length and in-plane velocities. In the next section it is moreover assumed that the collapse is initiated by yielding of the reinforcement, i.e., the membranes are plastified in yield regime I. For discontinuity lines of the velocity field that are compatible with yield regime I, the term collapse crack is used. Collapse cracks are straight lines. According to the flow rule for yield regime I, they must open normally to their direction.

2. COLLAPSE MECHANISMS FOR BEAMS IN TORSION, BENDING AND SHEAR

2.1 One-Dimensional Beam Theory

The derivation of yield criteria and flow rules for the differential beam element in terms of generalized stresses and strains (stress-resultants, curvature, twist, etc.) marks the transition from solid mechanics to one-dimensional beam theory. This transition is usually treated as a two-dimensional problem in the plane of a cross-section. Interaction relations are established through an investigation of possible states of stress and strain rates in a fully plastic cross-section. To this end simplifying assumptions with respect to the states of stress and deformation must always be made. The first usual assumption is that the transverse normal stresses, which do not enter the equilibrium conditions for a cross-section, are zero. The remaining assumptions are contained in the constitutive equations relating the stresses and strain rates in a cross-section to the generalized stresses and strain rates.

In the (static) truss model approach [1] it is assumed that the shear flow is constant along the perimeter of a thin-walled closed cross-section subjected to torsion or constant over the depth of a web subjected to shear. It is shown in Ref. [3] that these assumptions are consistent with the following kinematic assumptions for the deformed fully plastic cross-section.

- -the cross-sectional shape is not distorted
- -plane distribution of the longitudinal strain rates
- -warping of the cross-section out of its plane is unrestrained in the case of beams with closed, thin-walled cross-section subjected to uniform torsion and bending; warping of the web is unrestrained in the case of beams with single-symmetric thin-walled cross-section subjected to bending and shear.

Using these assumptions the corresponding interaction relations can also be found readily via the power of dissipation of the cross-section [3]. The resulting expressions for the distribution of the shear strain rates and for the warping function are completely analagous in form to those found in elastic beam theory for uniform torsion. While this sectional approach shows that the resulting interaction relations fully comply with usual assumptions of beam theory, it gives no indication under what conditions unrestrained warping can be assumed.

2.2 Spatial, Discontinuous Collapse Mechanisms

Due to the simplifying assumptions of the sectional approach, it is often not possible to find stress and velocity fields that satisfy the boundary, equilibrium and compatibility conditions of plane stress theory and that exhibit the stress and strain rate distribution found in the sectional approach. Indeed, for beams in bending and shear, it has been demonstrated in Ref. [3] that only the discontinuous collapse mechanisms shown in Fig. 3 can be associated with the generalized strains of the sectional approach. For beams in uniform torsion and bending such velocity fields exist, but they do not represent the shortest possible mechanisms, which are again discontinuous.

The mechanisms shown in Fig. 3 represent also the basic elements of the discontinuous collapse mechanisms for beams in torsion and bending with thin-walled closed cross-section of polygonal shape. Fig. 4a shows the basic torsional collapse mechanism for a beam with quadrilateral convex cross-section. The relation between the inclination of the skew axis of rotation AE and the inclinations of the collapse cracks ABC and EFG follows from the flow rule of perpendicular collapse crack opening and from the assumption that the beam ends undergo rigid body motion only. From kinematics it is easily found that the four collapse crack tips and the axis of rotation must lie in one plane. Assuming an unrestrained longitudinal extension of the mechanism, the same interaction relations result as from the (static) space truss model approach [2,3]. Each mechanism with axis of rotation in one of the four walls yields one interaction relation. If all longitudinal reinforcement is yielding at collapse, any linear combination of the four mechanisms is also feasible, in particular also a mechanism with pure twist and elongation as shown in Fig. 4b.

It is worthwhile to relate the kinematic assumptions for the spatial mechanisms to those of the more usual sectional approach. The assumption of a rigid body motion of the beam ends corresponds evidently to the assumptions of a plane distribution of the longitudinal strain rates and of no distortion of the sectional shape. In both approaches these assumptions ensure that the power of the external loads can be uniquely expressed in terms of the bending and torsional moments and the rates of curvature and twist or skew rotation, respectively. The assumption, finally, that the mechanisms of Fig. 4 can longitudinally spread in an unrestrained manner, corresponds to the assumption of unrestrained warping for a fully plastic cross-section. To illustrate the last statement, Fig. 5 shows a beam in uniform torsion with uniform stirrup reinforcement. The yield strength of the four longitudinal corner bars is Z_y within the test region L and much higher outside. The longitudinal distance between the points B and E, where the open collapse cracks cross the corner bars, is denoted by ℓ and the length that would develop in a uniformly reinforced beam by ℓ_u. For $\ell_u \leq L$, the mechanism is unrestrained, the shear flow is constant along the perimeter of the cross-section and the beam acts in pure St. Venant or uniform torsion. For $\ell_u > L$ the mechanism is restrained and a higher ultimate torque results. The exact collapse mechanism is characterized by $\ell = L$. The shear flow jumps at the corners, the forces in the corner bars vary (Fig. 5b) and, hence, the beam acts in nonuniform torsion.

It is common practice in reinforced concrete theory to treat solid cross-sections as box-sections, because test results have shown that solid and box-shaped beams with identical dimensions and reinforcement have practically the same ultimate torque. It is worthwhile therefore to investigate the collapse crack propagation into the core of the beam. Because the tips A, C, D, F of the two collapse cracks and the skew axis of rotation lie in one plane (Fig. 5a), collapse cracks propagate along the three planes ABC, DEF and ADCF into the core. While the collapse cracks ABC and DEF are externally visible, the collapse crack along

plane ADCF opens only internally thus creating a cavity. Assume that a skew bending crack opens along plane ADCF, while the front end of the beam rotates about axis AD (Fig. 5a). As shown in Fig. 6, the two crack edges are then in position ADCF' (Fig. 6a) and ADC'F (Fig. 6b). If the tetraeder ABCF rotates about axis AC from position ACF' into position ACF and the tetraeder CDEF about axis DF from position C'DF into position CDF, the skew bending crack is completely closed again along its perimeter. There remain the externally visible collapse cracks ABC, DEF and a cavity as shown in Fig. 6c. All the interior collapse crack surfaces are planes, and opening occurs everywhere normal to these planes. Consequently the core concrete does not contribute to the power of dissipation. Clearly, there is no difference in torsional resistance between box beams and solid beams with convex quadrilateral cross-sections, when failure is initiated by yielding of the reinforcement. In both cases only an outermost concrete layer is effective. This effective concrete layer, along with the reinforcement, is modelled in the present approach as a two-dimensional membrane. The membrane forces of the truss model and the in-plane velocity components of the mechanisms Figs. 4 to 6 are compatible and represent therefore an exact solution.

So far, only quadrilateral cross-sections have been treated. However, generalization to arbitrary, convex, polygonal thin-walled cross-sections is straightforward. Again, the basic mechanisms are characterized by a skew axis of rotation in one of the walls as shown in Fig. 7a. Any other mechanism compatible with yield regime I is a linear combination of such mechanisms. Starting from the skew axis of rotation, a sequence of overlapping collapse cracks forms that span over two walls (Fig. 7a and b). The relation between the inclination β of the axis of rotation and the inclinations α_i of the collapse cracks follows again from the flow rule of perpendicular collapse crack opening and from the assumption that the beam ends undergo rigid body motion only.

Consider the tip of the collapse crack starting at corner i. Due to the flow rule, the in-plane velocities $\dot{u}_i$, $\dot{v}_i$ must be related by (Fig. 7d)

$$a_i \dot{v}_i = L_i \dot{u}_i \tag{1}$$

Because the front end of the beam undergoes a rigid body motion only, the velocities in Eq. (1) are given by

$$\dot{u}_i = \dot{\omega} \sin\beta \; z_i \quad , \tag{2a}$$

$$\dot{v}_i = \dot{\omega} \cos\beta \; r_i - \dot{\omega} \sin\beta \; x_i \cos\delta_i \quad , \tag{2b}$$

where all terms are defined in Fig. 7. Finally, according to Fig. 7b, the length L_i of the mechanism in wall i is given by

$$L_i = x_i - x_{i-1} + a_i \cot\alpha_i + a_{i-1} \cot\alpha_{i-1} \tag{3}$$

Introducing Eqs. (2) and (3) in Eq. (1) and noting that $z_{i+1} = z_i + a_i \cos\delta_i$, there results the following recurrence formula for x_i.

$$z_{i+1} x_i = a_i r_i \cot\beta - z_i (a_i \cot\alpha_i + a_{i-1} \cot\alpha_{i-1}) + z_i x_{i-1} \tag{4}$$

Eq. (4) merely states that the skew axis of rotation and the crack tips in corner i and i+1 of wall i lie in one plane. Using Eq. (4) and starting with $x_i = 0$, the coordinates x_i of the front tips of each crack can be consecutively calculated. The condition that the last collapse crack must meet again the skew axis of rotation, finally yields

$$\cot\beta = \frac{1}{A_o} \sum_i \bar{z}_i \, a_i \cot\alpha_i \quad , \tag{5}$$

where A_o denotes the area enclosed by the cross-section and a_i, $\bar{z}_i$ are the depth and the z-coordinate of the middle line of wall i (Fig. 7d). For a beam with a regular polygonal cross-section and equal stirrup reinforcement in each wall the following simple relations hold: $\cot\beta = 2\cot\alpha$, $L_i = 2a\cot\alpha$. Using Eq. (5), again the interaction relations of the space truss model can be derived [3].

The derivation has only involved the in-plane velocities. A study including the velocity components normal to the walls reveals the following. The collapse cracks, the corner lines and the straight lines joining the crack tips (Fig. 7b) form the boundaries of the wall regions that move as rigid bodies. Contrary to quadrilateral sections, vectors of relative rotation are not only present in the lines joining the crack tips but moreover in the corner lines. The vectors of relative rotation between the crack edges point from the starting to the end point of the crack and have the same magnitude in both walls. Thus one collapse crack opens indeed along one plane.

3. PLANE STRESS PROBLEMS

The critical cross-sections are often located at points of applications of concentrated loads or at supports, where the simplifying assumptions of beam theory are hardly met. In deep beams the effect of shear transfer through strut action becomes significant. In these cases realistic theoretical values for the ultimate strength in bending and shear can only be expected from a plane stress approach that takes into account the variable concrete stress fields in the web. For underreinforced beams with variable depth the exact collapse mechanisms are basically the same as in Fig. 3. The corresponding concrete stress may vary, however, significantly over the depth of a cross-section. The mechanisms presented in the preceding section demonstrate that adjacent cross-sections can theoretically not be designed independently. In engineering practice, however, the needed reinforcement is always determined on a sectional basis. Thus the conditions have to be established, on which a sectional design ensures stable, statically admissible stress fields in the web.

These problems are treated in detail in Ref. [3] along with a discussion of the general stress and velocity fields in fully plastic reinforced concrete walls.

Fig. 8 summarizes some results of an investigation on possible concrete compression fields in a thin web near the base of a cantilever beam (Fig. 8a) and near a concentrated load (Fig. 8b). The web is assumed to be in yield regime I. The trajectories of the compression fields in the concrete form non-centered fans and are determined from the boundary condition of zero transverse normal stress along boundary AB and from the assumption that the concrete compressive strength is reached along boundary BC (Fig. 8a) or CD (Fig. 8b). Results are presented for several values for the ratio of the allowable nominal shear stress and the effective concrete strength, $\tau/\kappa\beta_p$, and for the selected inclination α_{dim} used to determine the stirrup reinforcement. The table in Fig. 8a shows that the additional longitudinal reinforcement needed in section BC due to the presence of shear may be of comparable order of magnitude as in the free span, although codes do usually not require such additional reinforcement in this case. The table in Fig. 8b presents values for the load transfer length e that is needed to ensure stable, statically admissible stress fields in the web below a concentrated load. These values may be of considerable magnitude. Clearly, these results show that further study is needed in this area.

Fig. 9 shows a deep beam after attainment of the ultimate load. A lower bound for the collapse load has been derived on the basis of the stress fields indicated in Fig. 9b [3]. The stirrups and the distributed longitudinal reinforcement are assumed to yield. The main longitudinal reinforcement is in tension

everywhere and reaches the yield strength in the points A and A'. The concrete compression field consists of a central strut and two non-centered fans. The concrete strength is reached in the strut and along the lines AC' and A'C. The experimental ultimate load was 174.5 kips or 85% of the theoretical ultimate load found from bending theory. The lower bounds derived from the stress fields as outlined above are 168 kips and 182 kips depending on whether the concrete cover of the reinforcement is assumed to be ineffective or effective, respectively. Neglecting the cover is equivalent to a 30% reduction in concrete strength. This reduction results only in a 8% decrease in the ultimate load. Theoretically approximately 30% of the shear force is carried by strut action. While this result indicates that the investigated stress fields may be realistic, realistic collapse mechanisms have still to be found.

4. CONCLUSIONS

The collapse mechanisms for beams in bending and torsion or bending and shear presented in this paper complete the (static) space truss model solution to an exact solution within the framework of a membrane theory as outlined above. In particular, they clarify the kinematic assumptions the resulting interaction relations are based on. This is of importance insofar as, first, conclusions with respect to the applicability of plastic theory can only be drawn from the comparison of test results with an exact or sufficiently bounded value for the theoretical collapse load. Second, kinematic assumptions can be verified more easily experimentally than static assumption.

The spatial mechanisms show that the warping term in the sectional approach reflects primarily the fact that the boundaries between rigid and yielding regions cannot lie in a cross-section normal to the beam axis. The finite length of the shortest possible mechanism implies that the interaction relations actually describe the strength of a whole beam region. This has to be kept in mind when detailing the reinforcement. The knowledge of the collapse mechanisms helps to detect weak reinforcing details. The finite length of the collapse mechanisms must also be appropriately considered in the analysis of test results and the design of test specimens. While the length of the mechanism is important for the reinforcement details, it is normally short compared to the beam length. This means that warping restraints have only a very localized effect. Such restraints have no effect at all on the strength of regions more distant than the minimal mechanism length.

Results from an investigation on the general stress fields in the web of beams and deep beam in bending and shear have been briefly summarized. They indicate that further work is needed on regions of application of concentrated loads and reactions and on deep beams. The lower bounds calculated for a deep beam exhibiting strut action indicate that the effort might be worthwhile.

ACKNOWLEDGEMENT

The reported results were obtained in the course of a research project under the supervision of Dr. B. Thürlimann, ETH Zürich, Switzerland.

REFERENCES

1. Thürlimann, B.: "Plastic Analysis of Reinforced Concrete Beams," IABSE Colloquium Kopenhagen 1979, Denmark, Introductory Report.
2. Mueller, P.: "Failure Mechanisms for Reinforced Concrete Beams in Torsion and Bending," Publications, International Association for Bridge and Structural Engineering (IABSE), Vol. 36-II, p. 147, 1976.

3. Mueller, P.: "Plastische Berechnung von Stahlbetonscheiben und -balken" (Plastic Analysis of Reinforced Concrete Shear Walls and Beams), Institut fur Baustatik und Konstruktion, ETH Zurich, Bericht Nr. 83, Birkhauser Verlag Basel und Stuttgart, 1978.

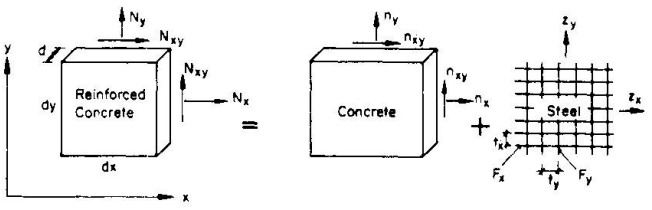

Fig. 1 Notation

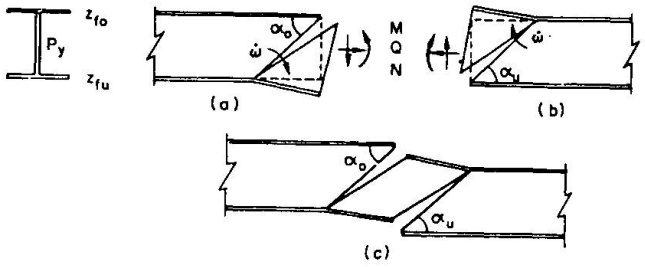

Fig. 3 Collapse Mechanisms for Underreinforced Beams in Bending and Shear

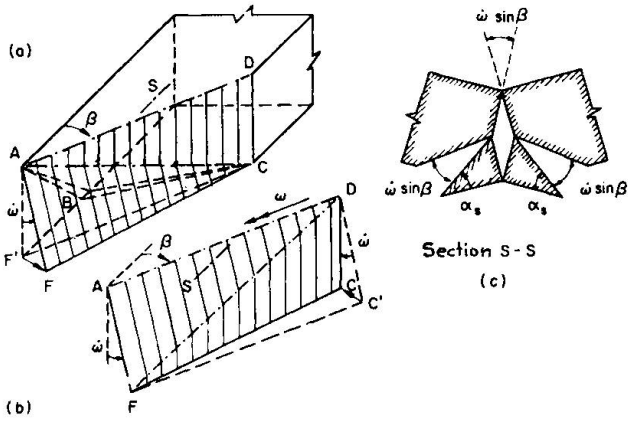

Fig. 6 Basic Torsional Mechanism for Solid Beams

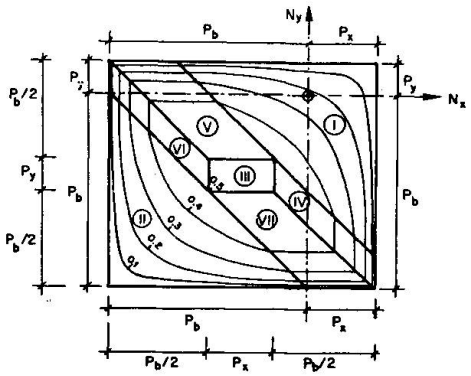

Fig. 2 Yield Criterion

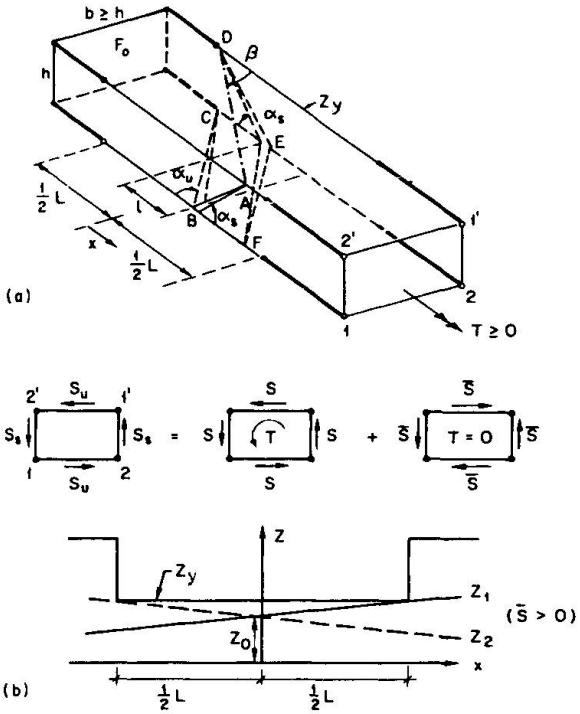

Fig. 5 Effect of Warping Restraints

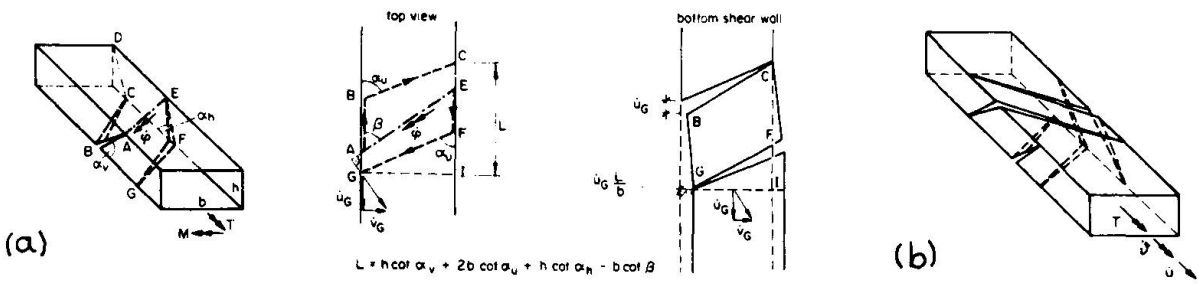

Fig. 4 Basic Torsional Collapse Mechanism (a) and Combined Mechanism (b)

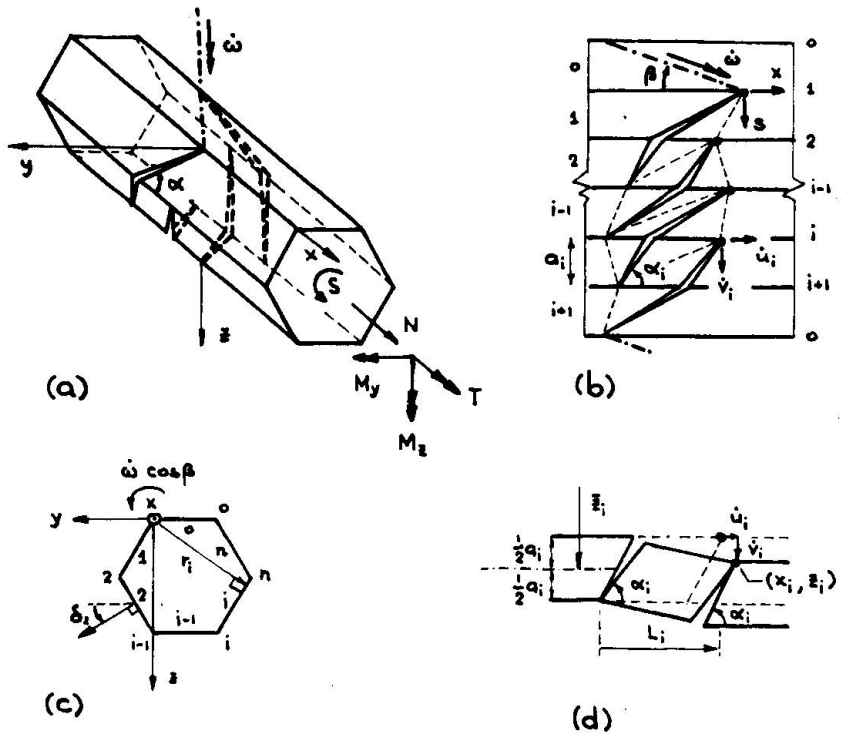

Fig. 7
Basic Torsional Mechanism for Beams with Polygonal Thin-walled Sections

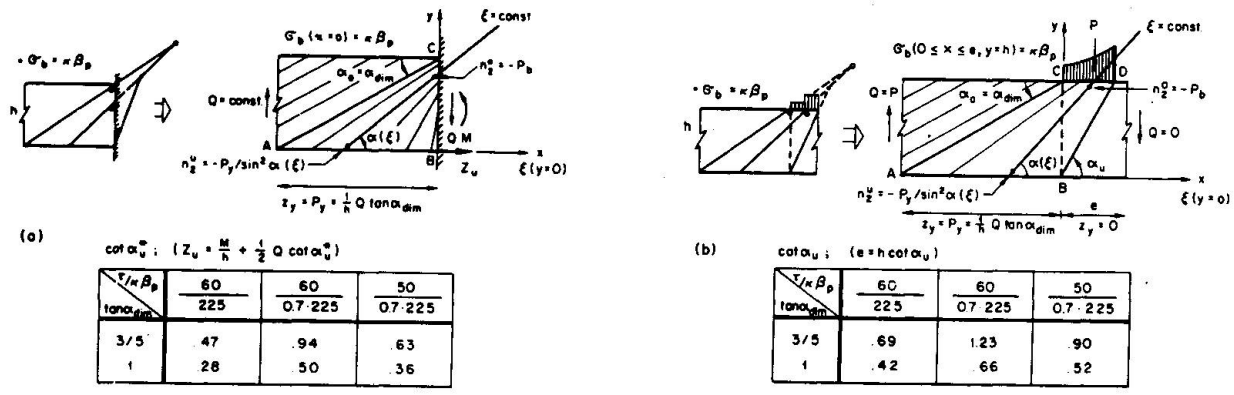

(a)

$\tau/\kappa\beta_p$ / $\tan\alpha_{dim}$	60/225	60/0.7·225	50/0.7·225
3/5	.47	.94	.63
1	.28	.50	.36

(b)

$\tau/\kappa\beta_p$ / $\tan\alpha_{dim}$	60/225	60/0.7·225	50/0.7·225
3/5	.69	1.23	.90
1	.42	.66	.52

Fig. 8 Stress Fields Near Support (a) and Concentrated Load (b)

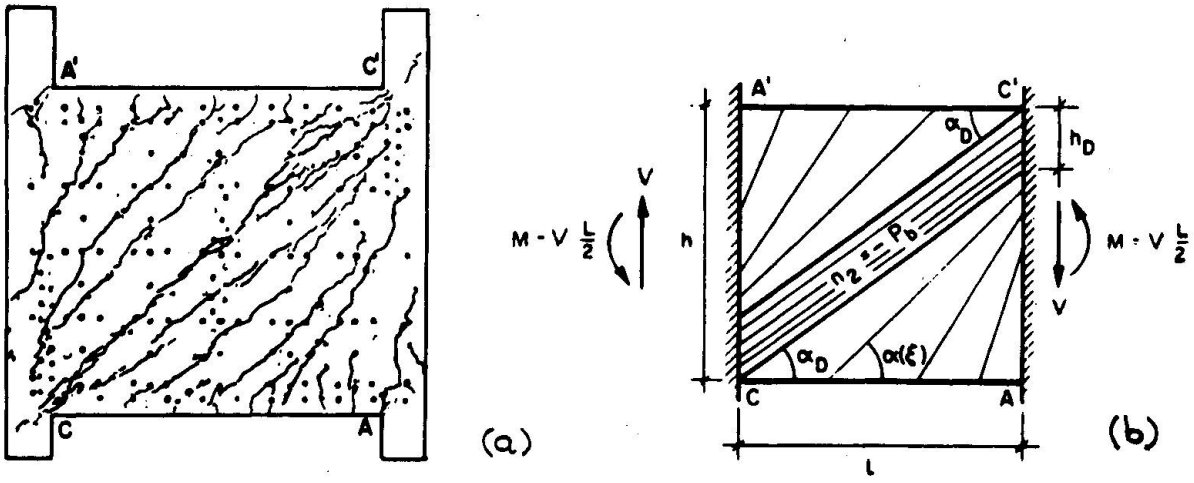

Fig. 9 Test Specimen of Deep Beam (a) and Investigated Stress Fields (b)

II

Torsion-Bending-Shear in Concrete Beams: A Kinematic Model

Poutres en béton armé soumises à la torsion, à la flexion et au cisaillement. Une solution cinématique

Torsion-Biegung-Schub in Stahlbetonbalken. Eine kinematische Lösung

L. ELFGREN
Associate Professor of Structural Engineering
University of Luleå
Luleå, Sweden

SUMMARY
A kinematic solution according to the theory of plasticity is presented for reinforced concrete beams loaded in combined torsion, bending and shear.

RESUME
La méthode cinématique de la théorie de la plasticité est appliquée pour déterminer la résistance des poutres soumises à la torsion, à la flexion et à l'effort tranchant.

ZUSAMMENFASSUNG
Für Stahlbetonbalken unter Torsion, Biegung und Querkraft wird eine Lösung nach der kinematischen Methode der Plastizitätstheorie dargestellt.

1. INTRODUCTION

A kinematic model for beams loaded in combined torsion and bending has recently been presented by Peter Müller and Bruno Thürlimann [1] - [3]. The model clarifies some contradictions in the theory for torsion which have earlier been discussed by the writer [4], [5].

In this paper the kinematic model of Müller-Thürlimann is extended to include the effect of vertical shear as well. The extension is based on the same principles as the writer has earlier used in a kinematic model for torsion-bending shear based on skew bending [4] - [9].

The presentation below follows the same outline as the one in Bruno Thürlimanns paper [1]. The same general assumptions are made i.e. the concrete and the reinforcement are rigid perfectly plastic materials. The concrete is governed by a square yield criterion. The reinforcement bars have a yield stress of $\pm f_y$ and carry forces in axial directions only. Local and bond failures are excluded.

2. KINEMATIC MODEL

A kinematic model for combined torsion, bending and shear is presented in Figs. 1 and 2. In Fig. 1 general notations are given and in Fig. 2 the kinematic model is presented. In the model, there are two cracks, ABC and DEF, see Fig. 2a. The right half of the beam rotates around the axis AD through the crack ends in the top of the beam. In the bottom of the beam a parallelogram, BCEF, is cut out. The rotation around the axis AD is notated $\dot{\omega}$. The rotation is possible if the axis AD is parallel to the diagonal CF in the paralleogram. This implies the condition that $\ell_{AD}=\ell_{CF}$, see Fig. 2b. Further, the angle β of the rotation axis AD follows from the following geometric conditions.

$$\ell_{CF} = b \cot \alpha_4 + h \cot \alpha_2 - \ell_{AD} + h \cot \alpha_6 + b \cot \alpha_4$$

With $\ell_{CF} = \ell_{AD}$ and $\cot \beta = \ell_{AD}/b$ we obtain

$$\cot \beta = \cot \alpha_4 + \frac{h}{2b} (\cot \alpha_2 + \cot \alpha_6) \qquad (2.1)$$

In order to express the energy dissipation, the velocity components of point B (equal to point E) are needed, see Fig.2c.

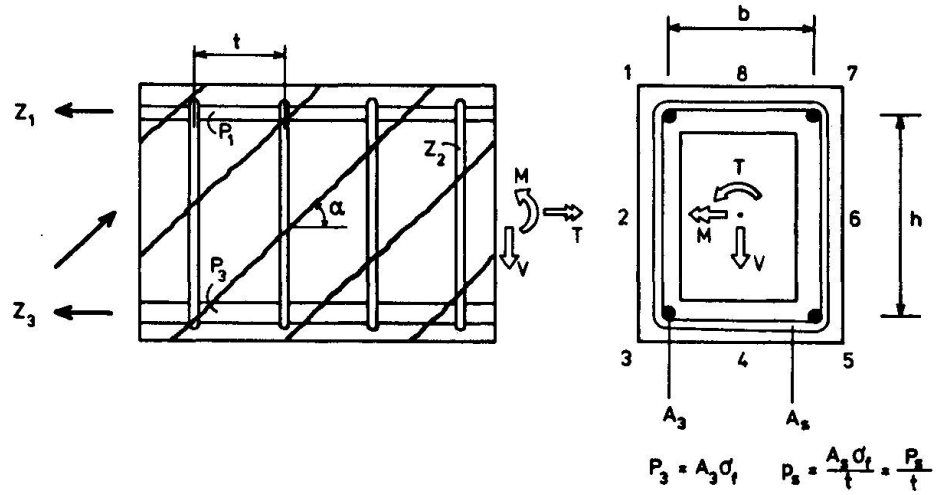

Fig. 1 Rectangular beam with box-section. Notations

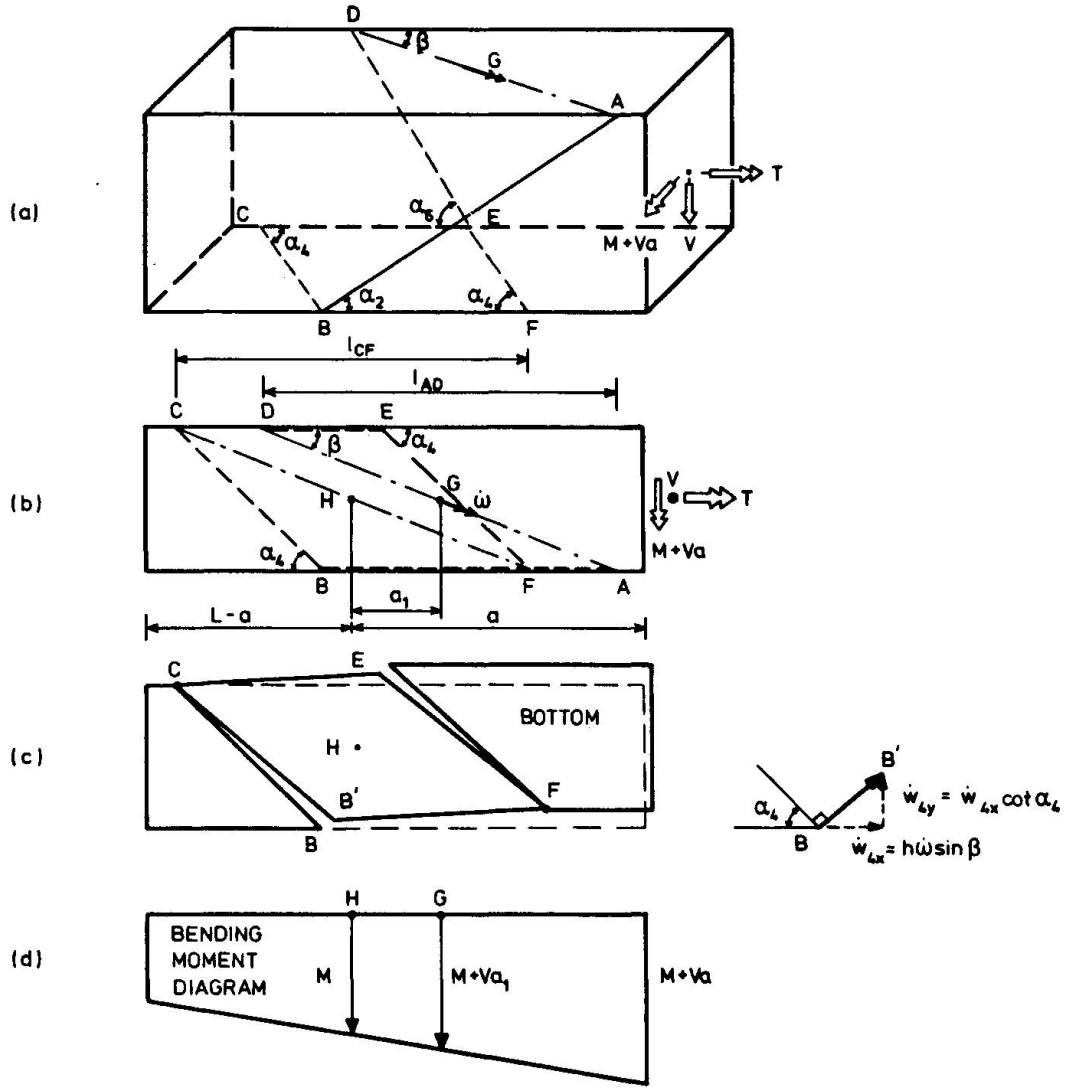

Fig. 2 Kinematic failure model: (a) General view; (b) Model seen from above; (c) Deformations in bottom; (d) Bending moment diagram.

$$\text{Wall 4:} \quad \dot{w}_{4x} = h\dot{\omega} \sin\beta \qquad \dot{w}_{4y} = \dot{w}_{4x} \cot\alpha_4$$
$$\text{Wall 2:} \quad \dot{w}_{2x} = h\dot{\omega} \sin\beta \qquad \dot{w}_{2y} = \dot{w}_{2x} \cot\alpha_2 \tag{2.2}$$

3. WORK EXPRESSIONS

Using the reinforcements shown in Fig. 1. the *internal work* in the cracks can be written as

$$L_{in} = \dot{w}_{4x}(P_3+P_5) + \tfrac{1}{2}p_s h\dot{w}_{2x} \cot^2\alpha_2 + p_s b\dot{w}_{4x}\cot^2\alpha_4 + \tfrac{1}{2}p_s h\dot{w}_{6x} \cot^2\alpha_6 \tag{3.1}$$

The *external work* carried out when the beam rotates around the axis AD can be written in the following way. As a vertical shear force, V, is present, the bending moment is varying. It has the value M at the reference point H in the middle of the bottom parallelogram, BCEF, see Fig. 2b, where the longitudinal reinforcement bars Nos. 3 and 5 are crossed by cracks. The distance in the longitudinal direction of the beam between the point H and the midpoint G on the rotation axis is a_1, and consequently the applied bending moment at point G will be $M + Va_1$. The external work equation then takes the form

$$L_{ex} = (M + Va_1)\ \dot{\omega} \sin\beta + T\ \dot{\omega} \cos\beta \tag{3.2}$$

where a_1 from Fig. 2b with cot β from Eq. (2.1) can be written as

$$a_1 = b \cot\alpha_4 + h \cot\alpha_2 - b \cot\beta = \frac{h}{2}(\cot\alpha_2 - \cot\alpha_6) \tag{3.3}$$

The failure mechanism is goverened by the three inclinations α_2, α_4 and α_6. In the general case these three angles are independent of each other. This general case is lengthy to handle. In order to simplify the deductions, the following assumption will be made regarding the relationship between the angles

$$\left.\begin{aligned} \cot\alpha_2 &= \cot\alpha_T + \cot\alpha_V \\ \cot\alpha_4 &= \cot\alpha_T \\ \cot\alpha_6 &= \cot\alpha_T - \cot\alpha_V \end{aligned}\right\} \tag{3.4}$$

The angles α_T and α_V are here two independent variables.

The assumption is motivated by the fact that the failure mechnism will in this way correspond with a probable stress distribution in the beam.

The expression for the internal work L_{in} in Eq. (3.1) can now be rewritten as

$$L_{in} = \dot{\omega} \sin \beta \left[h(P_3 + P_5) + \frac{1}{2}p_s h^2(2 \cot^2\alpha_T + 2 \cot^2\alpha_V) + p_s bh \cot^2\alpha_T\right] =$$

$$= \dot{\omega} \sin \beta[h(P_3 + P_5) + p_s h(b+h) \cot^2\alpha_T + p_s h^2 \cot^2\alpha_V] \qquad (3.5)$$

In order to simplify the expression for the external work L_{ex} in Eq. (3.2), we first rewrite the expression for cot β in Eq. (2.1) and the expression for the distance a_1 in Eq. (3.3)

$$\cot \beta = \cot \alpha_T + \frac{h}{2b} 2 \cot \alpha_T = \frac{b+h}{b} \cot \alpha_T \qquad (3.6)$$

$$a_1 = h \cot \alpha_V \qquad (3.7)$$

The external work can now be written

$$L_{ex} = \dot{\omega} \sin \beta[M + T \frac{b+h}{b} \cot \alpha_T + Vh \cot \alpha_V] \qquad (3.8)$$

The internal work in Eq. (3.5) shall be equal to the external work in Eq. (3.8)

$$M + T\frac{b+h}{b}\cot \alpha_T + Vh \cot \alpha_V = h(P_3+P_5) + p_s h(b+h)\cot^2\alpha_T + p_s h^2 \cot^2\alpha_V \qquad (3.9)$$

4. MINIMIZATION

If T and V are fixed, the minimum value of M with respect to the angles α_T and α_V follows from differentiations of Eq. (3.9) with respect to cot α_T and cot α_V

$$\frac{\partial M}{\partial \cot \alpha_T} + T \frac{b+h}{b} = 2p_s h(b+h) \cot \alpha_T$$

$$\frac{\partial M}{\partial \cot \alpha_V} = 0 \text{ gives } \cot \alpha_T = \frac{T}{2bh} \cdot \frac{1}{p_s} \qquad (4.1)$$

$$\frac{\partial M}{\partial \cot \alpha_T} + Vh = 2p_s h^2 \cot \alpha_V$$

$$\frac{\partial M}{\partial \cot \alpha_V} = 0 \text{ gives } \cot \alpha_V = \frac{V}{2h} \cdot \frac{1}{p_s} \qquad (4.2)$$

For the case of pure bending (T = V = 0), pure torsion (M = V = 0) and pure shear (M = T = 0), Eq. (3.9) with Eqs. (4.1) and (4.2) gives

$$M_0 = h(P_3 + P_5) \; ; \quad T_0 = 2bh\sqrt{\frac{P_3+P_5}{b+h}\,p_s} \; ; \quad V_0 = 2h\sqrt{\frac{P_3+P_5}{h}\,p_s} \tag{4.3}$$

Using Eqs. (4.1) to (4.3), Eq. (3.9) can now be rewritten as

$$M/M_0 + (T/T_0)^2 + (V/V_0)^2 = 1 \tag{4.4}$$

This is the same solution as has earlier been obtained with a static approach [4], [6], [10]. Hence ther is an identity between the kinematic model presented here and earlier presented static methods.

If the three inclinations α_2, α_4 and α_6 are retained as independent variables in the work expressions, Eq. (3.9) can be written in the following way.

$$M + T(\frac{h}{2b}\cot\alpha_2 + \cot\alpha_4 + \frac{h}{2b}\cot\alpha_6) + V\frac{h}{2}(\cot\alpha_2 - \cot\alpha_6) =$$

$$= h(P_3+P_5) + \frac{1}{2}p_s h^2(\cot^2\alpha_2+\cot^2\alpha_6) + p_s bh\cot\alpha_4 \tag{4.5}$$

A minimization of M with respect to the angles α_2, α_4 and α_6 will then give

$$\left.\begin{aligned} \cot\alpha_2 &= (\frac{T}{2bh} + \frac{V}{2h})\frac{1}{p_s} = \cot\alpha_T + \cot\alpha_V \\ \cot\alpha_4 &= \frac{T}{2bh}\cdot\frac{1}{p_s} = \cot\alpha_T \\ \cot\alpha_6 &= (\frac{T}{2bh} - \frac{V}{2h})\frac{1}{p_s} = \cot\alpha_T - \cot\alpha_V \end{aligned}\right\} \tag{4.6}$$

Hence, the shear flow from torsion and shear are acting in the same direction in side 2, and in opposite directions in side 4. This is in agreement with the assumption in Eq. (3.4).

5. DISCUSSION

The inter-action equation presented, Eq. (4.4), is deduced for point H in Fig. 2c. As can be seen from the moment diagram in Fig. 2d, the bending moment is higher in point G and in every point to the right of point H in the figure. The failure mechanism presented for point H is for this reason not stable [3].

A failure mechanism will start to develop in the area with the highest loads, that is, in the right end of the beam element in Fig.2. However, in the right end of the beam a support or a concentrated load may be situated. This will influence and change the failure mechanism. High concrete stresses will occur and they may cause the failure. For this reason the failure model will be more complicated in the vicinity of a support or a concentrated load.

To be correct according to the theory of plasticity, the effect of warping should be considered [3]. However, Paul Lüchinger has shown that for a rectangular beam, as is studied here, the effect of warping may be neglected [10]. If the warping is considered, it will at worst give a slightly higher load-carrying capacity.

Although the presented kinematic model is not stable for mispan cross-sections, it does give a rather good prediction of the type of cracks and deformations that has been observed in tests see Fig. 3 [7], [8]. The model also gives an identical load-carrying capacity as earlier presented static methods [4], [6], [10]. For these reasons, the writer considers the presented kinematic model to be a step in the direction of a better understanding of the interaction between torsion, bending and shear. To be able to give a complete solution to the problem, the effects of supports and of loading conditions must be studied. Here the concrete compression strength must be entered as an essential parameter.

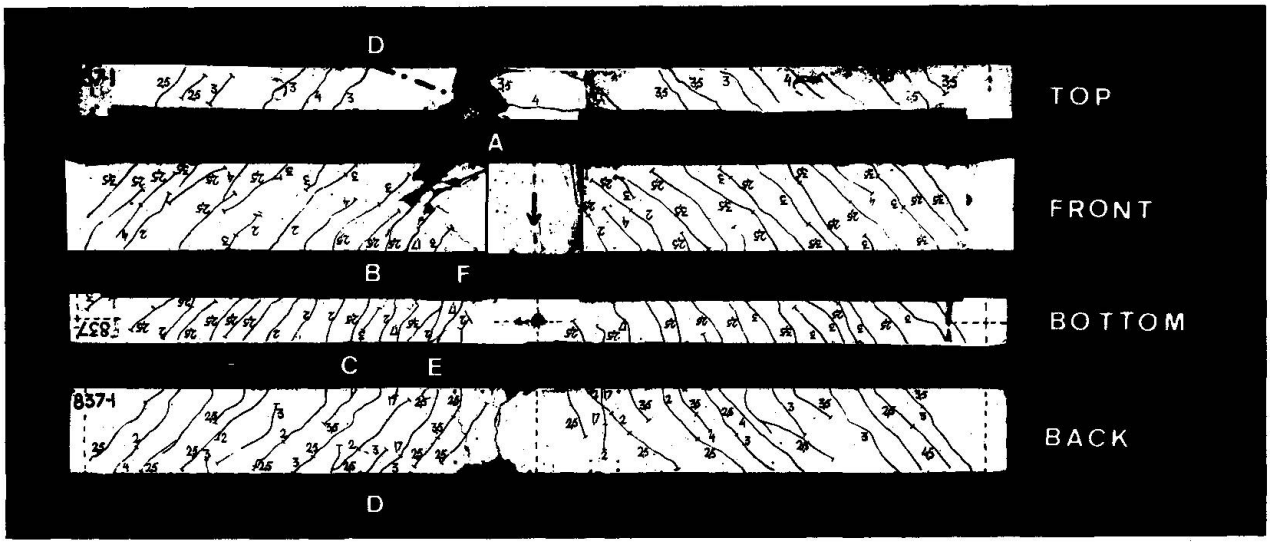

Fig. 3 Crack pattern and failure mechanism for a beam loaded in combined torsion, bending and shear. (Beam 1-1A in [4] and [7]). The beam is loaded in mid-span with an eccentric point-load acting downwards. The numerals along the cracks refer to the applied load when this part of the crack became visible (in Mp = MN/100). In the left part of the beam two failure cracks ABC and FED are indicated as well as a rotation hinge AD, compare with Fig. 2. (The beam is rectangular with $b \times h \times l$ = 100 x 200 x 3300 mm. The stirrup capacity is p_{s_T} = 0.236 MN/m. The relation between the bending moment M, the torsional moment T and the vertical shear force V in the failure section is M:T:Vh = 1:0.5:0.2).

REFERENCES

[1] BRUNO THÜRLIMANN: "Plastic Analysis of Reinforced Concrete Beams" IABSE Colloquium Kopenhagen 1979, "Plasticity in Reinforced Concrete", Introductory Report. Reports of the Working Commissions, International Association for Bridges and Structural Engineering (IABSE), Vol. 28, Zürich 1978, pp. 71-90.

[2] PETER MÜLLER: "Failure Mechanisms for Reinforced Concrete Beams in Torsion and Bending", Publications, International Association for Bridge and Structural Engineering (IABSE), Vol. 36-II, Zürich 1976, pp. 147-163

[3] PETER MÜLLER: "Plastische Berechnung von Stahlbetonscheiben und -balken" (Plastic Analysis of Walls and Beams of Reinforced Concrete), Institut für Baustatik und Konstruktion, ETH Zürich, Bericht Nr. 83, Birkhäuser Verlag, Basel und Stuttgart, 1978, 160 pp.

[4] LENNART ELFGREN: "Reinforced concrete beams loaded in combined torsion, bending and shear. A study of the ultimate load-carrying capacity". Dissertation, Chalmers University of Technology, Division of Concrete Structures, Publication 71:3, 1 Ed., Göteborg Nov. 1971, 204 pp, revised 2nd Ed., Göteborg Aug. 1972, 230 pp.

[5] LENNART ELFGREN - INGE KARLSSON - ANDERS LOSBERG: "Nodal forces in the analysis of the ultimate torsional moment for rectangular beams". Magazine of Concrete Research (London), Vol 26, No 86, March 1974, pp 21-28.

[6] LENNART ELFGREN - INGE KARLSSON - ANDERS LOSBERG: "Torsion - bending - shear interaction for reinforced concrete beams". Journal of the Structural Division, American Society of Civil Engineers (ASCE) (New York), Vol 100, No ST 8, Proc. Paper 10749, August 1974, pp 1657-1676.

[7] LENNART ELFGREN - INGE KARLSSON: "Tests on rectangular beams in combined torsion, bending and shear". Chalmers University of Technology, Division of Concrete Structures. Report 71:1, Göteborg Nov 1971, 128 pp.

[8] INGE KARLSSON - LENNART ELFGREN: "Förespända lådbalkar belastade med vridande och böjande moment samt tvärkraft" (Torsion, bending, and shear in Prestressed Concrete Box Girder Beams). Chalmers University of Technology, Division of Concrete Structures, Report 76:10, Göteborg, Sept 1976, 88 pp.

[9] A A GVOZDEV - N N LESSIG - L K RULLE: "Research on Reinforced Concrete Beams under Combined Bending and Torsion in the Soviet Union". Paper SP 18-11 in "Torsion of Structural Concrete", American Concrete Institute (ACI), Publication SP-18, Detroit 1968, pp 307-336.

[10] PAUL LÜCHINGER: "Bruchwiderstand von Kastenträgern aus Stahlbeton unter Torsion, Biegung und Querkraft" (Ultimate Strength of Box-Girders in Reinforced Concrete under Torsion, Bending and Shear), Institut für Baustatik und Konstruktion, ETH Zürich, Bericht Nr. 69, Birkhäuser Verlag, Basel und Stuttgart, 1977. 107 pp.

II

Reinforced Concrete Members in Torsion and Shear

Eléments en béton armé soumis à la torsion et au cisaillement

Stahlbetonelemente in Torsion und Schub

M.P. COLLINS
Professor
University of Toronto
Toronto, Canada

SUMMARY
Progress in developing a rational model (the diagonal compression field theory) capable of predicting the behaviour of reinforced concrete members in torsion and shear is reported. The differences between the diagonal compression field theory and the procedures based on plastic analysis are highlighted.

RESUME
Cet article rend compte du progrès dans le développement d'un modèle rationnel (théorie du champ de compression diagonale) capable de prédire le comportement d'éléments en béton armé soumis à la torsion et au cisaillement. Les différences entre la théorie du champ de compression diagonale et les méthodes de l'analyse plastique sont mises en évidence.

ZUSAMMENFASSUNG
Es wird über den Fortschritt bei der Entwicklung eines rationalen Modells (Theorie des diagonalen Druckfeldes) berichtet, mit dem das Verhalten eines Stahlbetonelementes bei Torsion und Schub vorausgesagt werden kann. Die Unterschiede zwischen der Theorie des diagonalen Druckfeldes und den Verfahren, die auf plastischen Berechnungen beruhen, werden herausgestellt.

1. INTRODUCTION

During the past 10 years research aimed at developing behavioural theories for reinforced concrete in torsion and shear comparable in rationality and generality to the well known theory for flexure and axial load has been conducted at the University of Toronto.

The unsatisfactory nature of the shear and torsion "theories" currently used in North American design practice is evident if the ACI [1] chapter on shear and torsion is compared with the ACI chapter on flexure and axial load. In the flexure and axial load chapter a rational, simple, general method is explained in a few paragraphs of text. On the other hand, the shear and torsion chapter consists of a collection of complex, restricted, empirical equations which, while leading to safe designs if properly used, lack any understandable central philosophy. This lack, in the opinion of the author, is the source of many of the complaints which arise from the profession about modern design codes becoming unworkably complicated.

In this paper first the well known theory for flexure and axial load will be briefly reviewed. Then the development of comparable theories for pure torsion, torsion and bending, and shear and bending will be summarized. The paper will conclude by contrasting the theories developed at Toronto with those developed in Zurich and Copenhagen.

2. PLANE SECTIONS THEORY FOR FLEXURE AND AXIAL LOAD

Although the "plane sections" theory which is capable of predicting the behaviour of reinforced concrete beams loaded in flexure and axial load is fully described in many textbooks (e.g. [2]) it will be briefly illustrated here so that the capabilities of the theory, and the assumptions on which it is based can be more readily appreciated.

Assume that it is desired to find the moment-curvature relationship of a rectangular reinforced concrete beam from the known cross-sectional dimensions, Fig. 1(a), and the known stress-strain characteristics of the concrete, Fig. 1(b), and the steel, Fig. 1(c). As it is assumed that "plane sections remain plane" only two variables (say the concrete strain at the top, ε_{ct}, and the depth to the neutral axis, kd) are required to define the concrete longitudinal strain distribution, Fig. 1(d). For a chosen value of ε_{ct} a trial value of kd can be selected and the concrete strain distribution will then be fixed. The longitudinal concrete stresses, Fig. 1(e), can then be found from the concrete strains by using the assumed concrete stress-strain characteristics. Usually it is assumed that in compression the stress-strain curve obtained from a test cylinder, Fig. 1(b), can be used and that in tension the concrete is not capable of resisting stress. To determine the steel stress it is assumed that the strain in the steel is equal to the strain in the surrounding concrete, Fig. 1(d), and that the stress-strain characteristics obtained from a tension test of a reinforcing bar, Fig. 1(c), can be used. Knowing the stresses acting on the cross-section the resulting compression force in the concrete, C, and tension force in the steel, S, can be computed, Fig. 1(f). In the case of zero axial load, equilibrium requires that C equals S and so if this is not the case the trial value of kd must be adjusted and the calculations repeated. When the correct value of kd has been found the moment, M, corresponding to the chosen value of ε_{ct} can then be calculated,

Fig. 1(g). This moment along with the curvature calculated from the strain distribution, Fig. 1(d), will give one point on the moment-curvature plot. Repeating the calculations for different values of ε_{ct} will produce the complete moment-curvature relationship, Fig. 1(h).

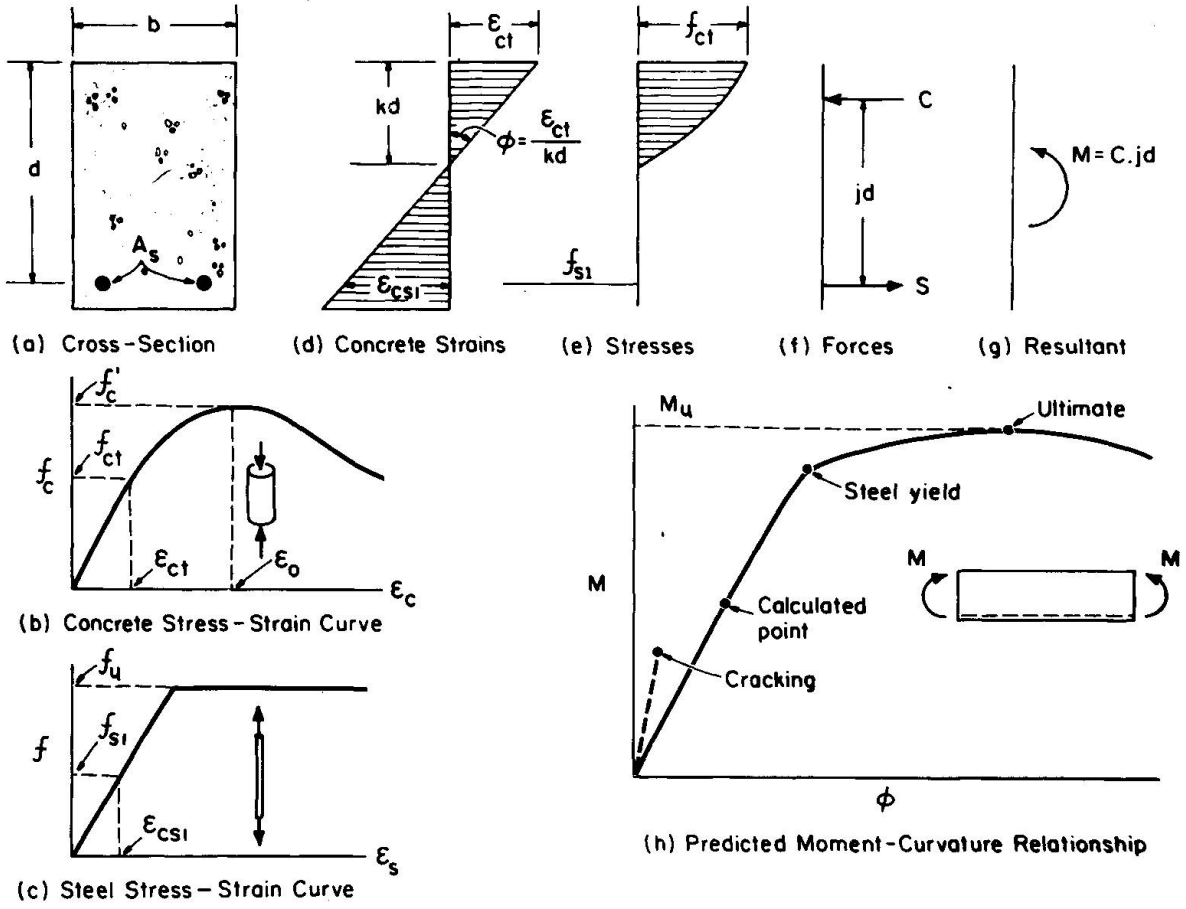

Fig. 1 Plane Sections Theory for Flexure

It should be noted that the concrete strains used in the above calculations are "average" strains rather than actual local strains. Thus the tensile strain at the level of the steel, ε_{csi}, will be the average of high local values that will occur at crack locations and the lower values that will occur between the cracks. In a similar fashion the calculated steel stress, f_{si}, should be representative of the average stress in the steel.

In determining the magnitude and position of the resultant compression in the concrete, C, Fig. 1(f), it is sometimes convenient to replace the actual stress distribution with an equivalent uniform stress distribution. Thus the distribution shown in Fig. 1(e) could be replaced by a uniform stress of $\alpha_1 f'_c$ acting over a depth β_1 kd where the stress block factors α_1 and β_1 have been chosen so that the magnitude and position of C do not change. For a constant width of beam, b, the values of α_1 and β_1 will depend only on the shape of the stress-strain curve, Fig. 1(b), and the value of the highest concrete strain, ε_{ct}.

The simple "plane sections remain plane" theory illustrated in Fig. 1 can be applied to quite complex problems. For example, Fig. 2 compares the predicted [2] moment-curvature response of a reinforced concrete beam subjected to reversed, cyclic loading with the experimentally determined response. Apart from the plane sections theory, only the stress-strain characteristics of the concrete and the steel under reversed, cyclic loading were required to make this prediction.

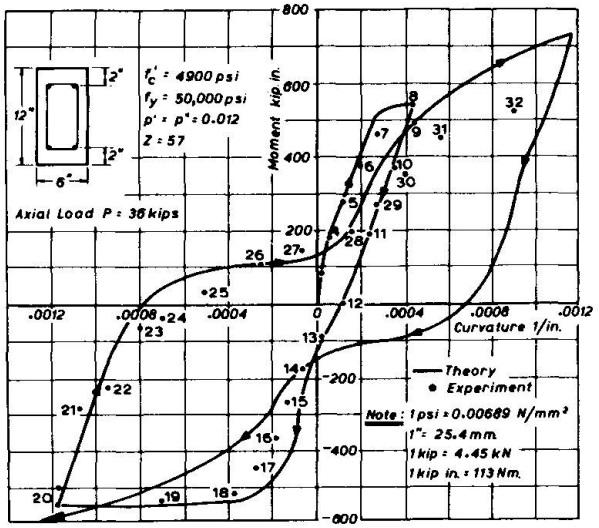

Fig. 2 Predicted Moment-Curvature Response Under Reversed Cyclic Loading [2]

3. DIAGONAL COMPRESSION FIELD THEORY FOR PURE TORSION

The diagonal compression field theory for pure torsion, which has been presented in more detail elsewhere [3], will be illustrated here by examining the problem of predicting the post-cracking torque-twist response of symmetrically reinforced concrete beams.

The theory assumes that after cracking the concrete can carry no tension and that the torsion is resisted by diagonal concrete compressive stresses which spiral around the beam at a constant angle α, Fig. 3(a). The outward thrust of these diagonal compressive stresses tends to push the corners of the beam apart which produces tension in the transverse hoops. The longitudinal components of the diagonal compressive stresses tends to push apart the ends of the beam which produces tension in the longitudinal steel.

Not all of the concrete is effective in providing diagonal compressive stresses to resist the torsion. The concrete cover outside of the hoop centreline is assumed to be ineffective because at higher loads this cover will spall off [3]. If the deformed shape of the twisted beam, Fig. 3(b), is examined it can be observed that the walls of the beam do not remain plane surfaces. Because of the curvature of the walls, ϕ_d, the diagonal compressive strains will have their maximum values at the surface, ε_{ds}, and will decrease linearly with the distance from the surface becoming tensile for depths below a certain distance, t_d. Thus in torsion as in flexure we have a depth of compression below which we may assume that the concrete, being in tension, is ineffective. The outside concrete spalls off and the inside concrete goes into tension, hence we are left with a tube of effective concrete t_d thick which lies just inside the hoop centreline.

The diagonal concrete stresses will vary in magnitude over the thickness of the effective concrete tube from zero at the inside to a value f_{ds} corresponding to

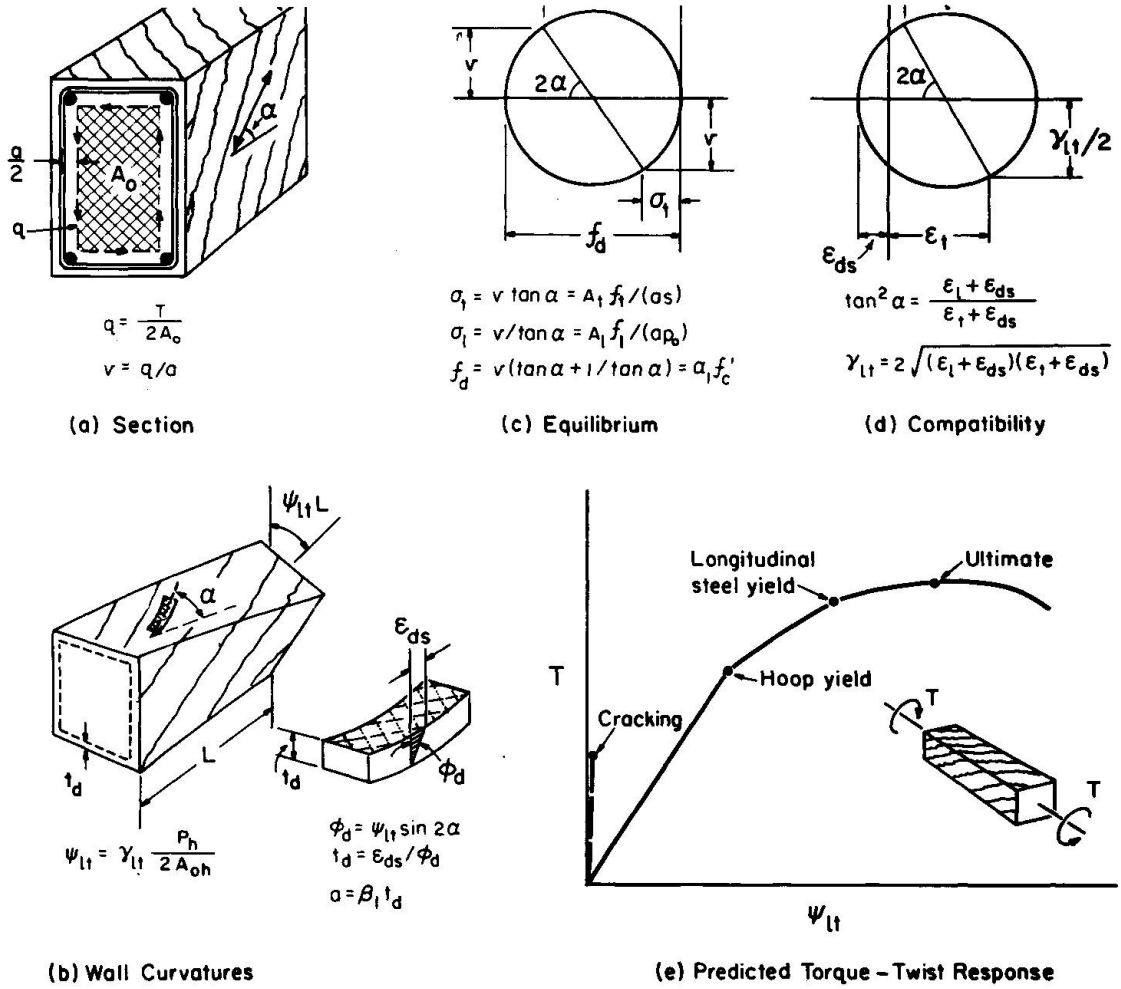

Fig. 3 The Diagonal Compression Field Theory for Pure Torsion

the strain ε_{ds} at the effective outside surface. As in flexure we can replace this actual stress distribution by a uniform stress of $\alpha_1 f_c'$ acting over a depth of $\beta_1 t_d = a$ the stress block factors α_1 and β_1 depend on the shape of the concrete stress-strain curve and the value of ε_{ds}. The depth of this uniformly stressed concrete, a, will define the path of the shear flow, q, Fig. 3(a) and hence the terms A_o (the area enclosed by the shear flow) and p_o (the perimeter of the shear flow path).

To illustrate how a solution can be obtained let us imagine that we wish to find the response of a given beam to a given torsional load, T. We could start by estimating the equivalent depth of compression, a. From a and the known hoop geometry we could find A_o and p_o, Fig. 3(a) and then from T, A_o and a, the uniform shear stress, v, could be found. After a trial value for the angle of inclination of the principal compressive stress, α, has been chosen we can use the equilibrium equations, Fig. 3(c), to find the stresses in the transverse hoop steel, f_t, the longitudinal steel, f_ℓ, and the equivalent uniform diagonal stress in the concrete, f_d. These stresses and the appropriate stress-strain curves for the concrete and the steel, e.g. Fig. 1(b) and 1(c), can then be used to determine the tensile strains in the hoop steel, ε_t, and the longitudinal steel, ε_ℓ, and the compressive diagonal surface strain of the concrete, ε_{ds}. These strain values enable the direction of the principal

compressive strain to be computed, Fig. 3(d), and hence allow the trial value of α to be checked. It is assumed that the direction of principal compressive stress coincides with the direction of principal compressive strain. After a consistent value of α has been found the strain values can be used to compute the twist of the beam, $\Psi_{\ell t}$, Fig. 3(b), (A_{oh} and p_h are the area enclosed by the centreline of the hoop and the perimeter of this area, respectively.) Once the twist is known the curvature of the walls, ϕ_d, can be calculated, Fig. 3(b). This curvature and the surface strains, ε_{ds}, define the equivalent depth of compression, a, Fig. 3(b). If the calculated value of a does not agree with the assumed value then a new estimate of a must be made and the calculations repeated. When the correct value of a has been determined then the response of the beam (i.e. the twist and the strains) at this given value of torque will have been found.

While the calculations described above perhaps sound rather formidable, it is possible to reformulate the expressions so that only one variable has to be found by trial and error [3]. With the aid of a programmable pocket calculator the complete torque-twist curve of a beam, Fig. 3(e), can then be found in about the same time as it takes to find the moment-curvature curve, Fig. 1(h).

4. COMBINED TORSION, FLEXURE AND AXIAL LOAD

The recently developed [4] compression field theory for combined torsion, flexure and axial load is essentially a combination of the plane sections theory for flexure and the diagonal compression field theory for torsion. The theory will be illustred here by discussing the manner in which the response of a beam loaded in combined torsion and flexure can be predicted.

Say that we wish to find the response of a given beam, Fig. 4(a), to a given torsional load, T, and a given flexural load, M. As in flexure the longitudinal strain distribution will be defined by two variables, Fig. 4(b) which this time we will choose as the top strain, ε_{ct} and the bottom strain, ε_b. The calculations commence by estimating ε_{ct} and ε_b. From the estimated strain distribution and the stress-strain curve of the steel the magnitude and position of the resultant tension force in the longitudinal steel, S, can be calculated, Fig. 4(e).

For any element of concrete the longitudinal stress depends not only on its longitudinal strain and stress-strain curve but also on the magnitude of the coexisting shear stress. If tension is to be avoided then when shear stresses are present there must also be longitudinal compressive stresses even when there are longitudinal tensile strains, Fig. 3(c) and Fig. 3(d). Given the shear stress, the longitudinal strain, the amount of transverse steel and the stress-strain curves, the longitudinal concrete stress can be calculated. For convenience the beam section can be divided into elements so that within each element the longitudinal strain can be taken as approximately constant, Fig. 4(a). As in the pure torsion calculations there will be a tube of effective concrete lying just inside the hoop centreline but now the thickness of the tube will vary around the cross-section. For each element an estimate is made of this thickness (i.e. the equivalent depth of compression) and from these estimates A_o and hence the shear stresses, v, in each element are calculated, Fig. 4(a). For each element an estimate is then made of the angle of inclination of the principal stress, α. Knowing α and v the transverse hoop strain ε_t and the diagonal concrete strain ε_{ds} can be calculated from the equilibrium equations of Fig. 3(c) and the stress-strain curves of Fig. 1(b) and Fig. 1(c). The estimate of α can

then be checked from the basic geometric equation of Fig. 3(d), namely:

$$\tan^2\alpha = \frac{\varepsilon_\ell + \varepsilon_{ds}}{\varepsilon_t + \varepsilon_{ds}} \qquad \ldots\ldots (1)$$

When α values satisfying Eq.(1) have been found then the longitudinal concrete compressive stresses, σ_ℓ, can be calculated for each element, Fig. 4(d), and from these the position and magnitude of the resultant concrete compressive force, C, can be determined, Fig. 4(e).

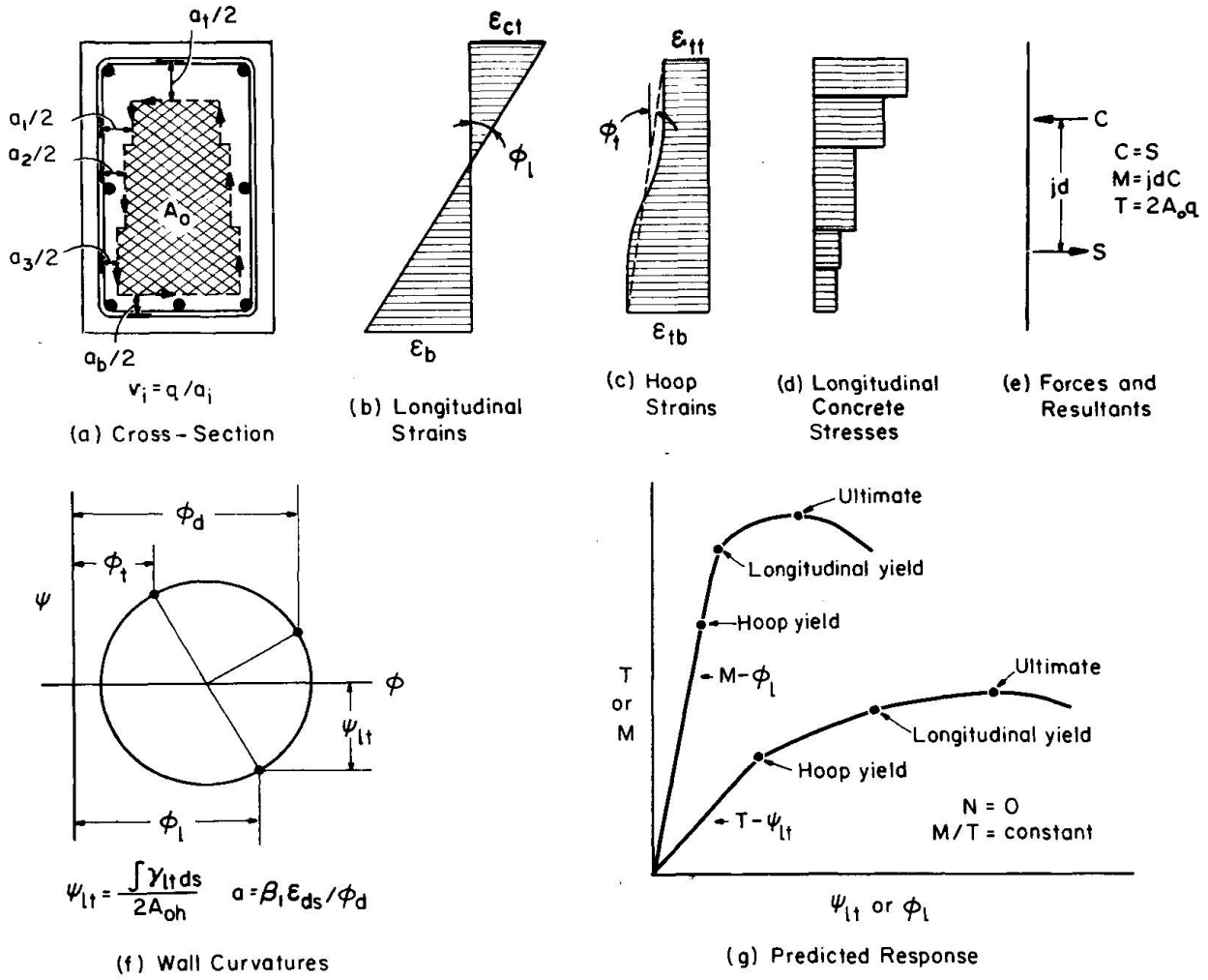

Fig. 4 The Diagonal Compression Field Theory for Torsion and Flexure

As well as giving the force C the calculations described above will have produced the distributions of transverse hoop strains, Fig. 4(c), and diagonal concrete strains around the section. These will enable the shear strains, Fig. 3(d), and hence the twist of the beam to be evaluated. From the twist, $\psi_{\ell t}$, the longitudinal curvature, ϕ_ℓ, and the transverse curvature, ϕ_t (the top and bottom faces of the beam will be curved transversely) the diagonal curvature, ϕ_d, can be calculated, Fig. 4(f). For each element ϕ_d and ε_{ds} enable the thickness a to be calculated, Fig. 4(f). If the calculated values of a do not

agree with the assumed values then new estimates must be made and the calculations repeated. When the correct values of a have been found then the axial force, N, and moment, M, corresponding to the assumed longitudinal strain profile can be determined from the magnitudes and positions of the forces C and S, Fig. 4(e). If N and M do not have the desired values (in our case N should equal zero and M should equal the given value) then a new longitudinal strain profile is chosen and the whole process is repeated.

While the trial and error procedure described above sounds very laborious it luckily converges very rapidly and hence with the aid of a programmable calculator or a small computer the moment-curvature and torque-twist curves, Fig. 4(g) can be obtained relatively easily.

5. COMBINED SHEAR, FLEXURE AND AXIAL LOAD

The compression field theory has been applied to the loading cases of shear [5] and shear combined with flexure and axial load [6]. As might be expected the procedures are very similar to those for torsion and torsion and flexure. These procedures will be illustrated here by discussing the manner in which the response of a beam loaded in combined shear and flexure can be predicted.

Say that for a given beam, Fig. 5(a), we wish to find the deformations and strains associated with a given shear load, V, and a given flexural load, M. Once again the calculations commence by estimating the longitudinal strains ε_{ct} and ε_b, Fig. 5(b), from which the magnitude and position of the resultant tension force, S, in the longitudinal steel can be calculated, Fig. 5(e).

The beam is again divided into elements (this time full width strips) so that within each element the longitudinal strain can be taken as constant, Fig. 5(b). In torsion the effective width, a, was initially unknown but once we had assumed a the shear stress could be directly calculated, Fig. 4(a). In shear the width of the strips, b, is known (the side cover is again assumed to be ineffective) but the relative magnitudes of the shear stresses in the various strips can not be directly calculated. We need to make an initial estimate of the shear stress distribution, Fig. 5(c), which should of course satisfy the basic equilibrium requirement that the integral of the shear stresses over the total area must equal the shear force, V. As in the case of torsion and flexure once we know the longitudinal strain, ε_ℓ, and the shear stress, v, in a given element we can calculate the longitudinal concrete compression, σ_ℓ. From the values of σ_ℓ, Fig. 5(d), the magnitude and position of the resultant compression in the concrete, C, can be calculated, Fig. 5(e) and hence the axial load, N, and moment, M, can be determined, Fig. 5(e), and compared with the desired values.

How do we check the assumed shear stress distribution? To do this we examine a section of the beam a small distance, Δx, away from the original section, Fig. 5(f). The longitudinal strain distribution and the steel concrete stresses corresponding with the loads at this new section must be found. With the longitudinal stress distributions for these two sections known the shear stress at any depth can be calculated, Fig. 5(g). If the calculated shear stress distribution does not agree with the assumed distribution then the whole process is repeated.

Once again the trial and error procedure described above converges very rapidly and hence the predicted response (e.g. the relationship between the applied shear and the maximum hoop strain, Fig. 5(h)) can be obtained relatively easily.

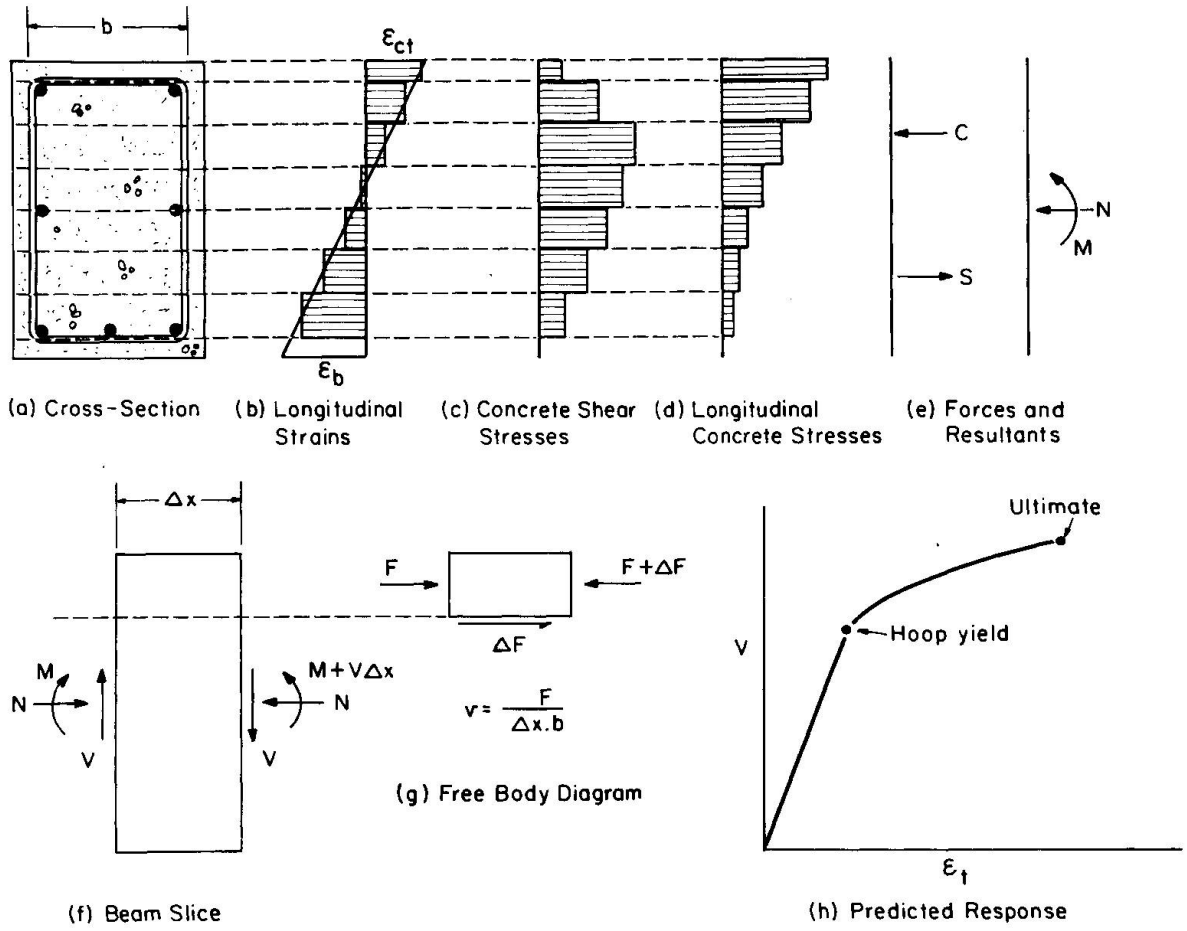

Fig. 5 The Compression Field Theory for Shear and Flexure

However, if the stress-strain curve for the diagonally cracked concrete is assumed to be the same as that obtained from a cylinder test, Fig. 1(b), the failure load of the specimen will be overestimated. While the more promising approach appears to be the modification of the stress-strain curve to allow for shear strains [7] the present procedure is to empirically limit the magnitude of the principal diagonal compressive stress, f_d, to a value f_{du} given by:

$$f_{du} = \frac{3.6\ f'_c}{1 + 2\ \gamma_m/\varepsilon_o} \qquad \ldots\ldots\ (2)$$

where γ_m is the maximum shear strain, $\varepsilon_\ell + \varepsilon_t + 2\ \varepsilon_{ds}$, and ε_o is the cylinder peak stress strain, Fig. 1(b).

6. THE DIAGONAL COMPRESSION FIELD THEORY AND PLASTIC ANALYSIS

The plastic analysis procedures for reinforced concrete beams in torsion and shear developed in Zurich [8] and Compenhagen [9] are concerned with predicting the failure loads whereas the compression field theory summarized above attempts to predict the complete load deformation response of the beams. Even if concern is restricted to only failure load predictions there are a number of singificant differences between the two approaches. Some of these differences will be illustrated below.

Shown in Fig. 6 is the observed relationship between failure torque and amount of reinforcement for 6 beams (M1 - M6) tested by Hsu [10]. For all these beams the concrete strength (28 MPa) and the steel strength (330 MPa) remained essentially constant and the volume of longitudinal steel was 1.5 times the volume of hoop steel. For small amounts of steel (Beams M1 and M2) both the hoop steel and the longitudinal steel yielded at failure. For larger amounts of steel (Beams M3, M4 and M5) only the hoops yielded at failure while for very large amount of steel (Beam M6) the beam failed before any steel yielded. As can be seen from Fig. 6 the failure torques and manner of failure for these beams are predicted well by the compression field theory.

Also shown in Fig. 6 are the failure torques predicted for these beams by the provisions of the new CEB Code [11]. These code equations are based on the Zurich plastic analysis procedures. The CEB equations which assume that all the steel yields at failure of course become unconservative when the steel does not yield at failure. However, the empirical equation which is intended to predict failures in which the concrete crushes before the steel yields is very conservative for these beams. What is more, it predicts that as the amount of reinforcing steel is increased the torsional capacity will be decreased. This happens because for these beams the amount of steel was increased (for M1 - M5) by increasing the size of the reinforcing bars which had the effect of decreasing the distance between the centres of the corner longitudinal bars and for this method A_o (the area enclosed by the shear flow) is defined as the area enclosed by lines joining the centres of the corner longitudinal bars.

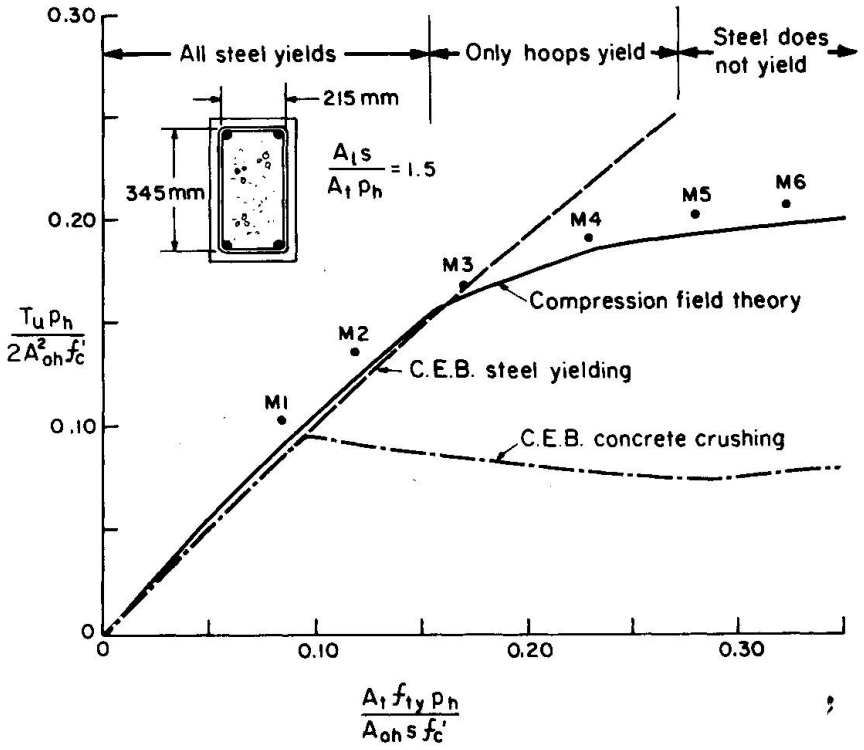

Fig. 6 Torsional Capacity versus Amount of Reinforcement

To summarize, the compression field theory can predict the strains at failure, the area enclosed by the shear flow, A_o, the effective wall thickness of the wall, a, the angle of principal compression, α, and the failure torque, T_u. The plastic analysis procedures must assume the area A_o, and the wall thickness, a, and can only accurately predict α and T_u if all of the steel is yielding.

As a final point, Fig. 7 illustrates the effect of prestress on shear strength. The results of four beams (SP0 - SP3) tested by Sadler [12] all of which had the

same reinforcement are shown. The main variable between these four beams was the magnitude of the uniform precompression, σ, that was applied by the unbonded central Dywidag bars.

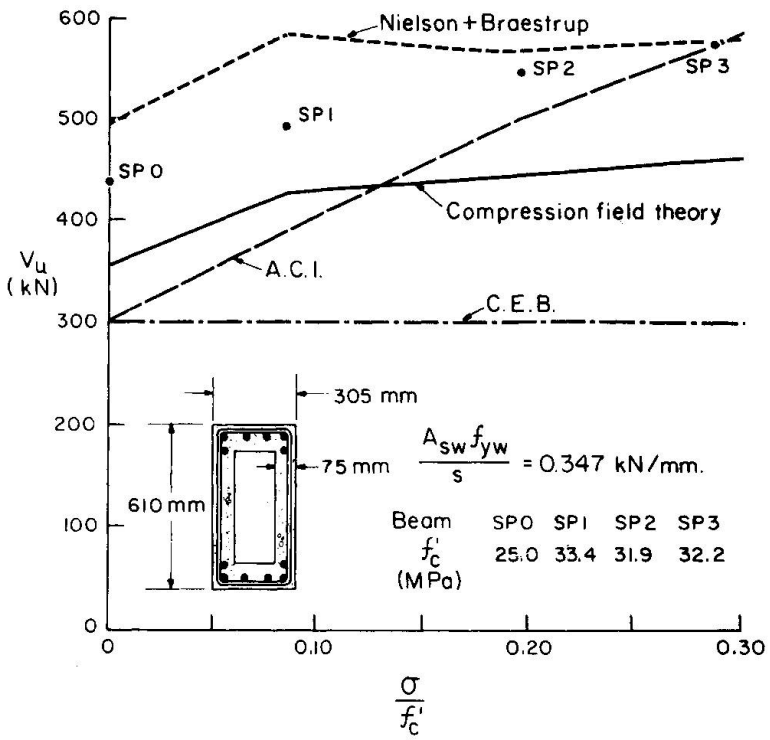

Fig. 7 Shear Capacity versus Level of Prestress

The plastic analysis procedures developed by Neilson and Braestrup [9] predict that prestressing should not influence the shear capacity and that Beam SP1 having the highest concrete strength, Fig. 7, should have the highest shear capacity. The CEB predictions [11] for these beams as well as not being influenced by the magnitude of the prestress are not influenced by the concrete strength hence all four beams are predicted to have the same strength.

In direct contradiction to the plastic analysis procedures the ACI Code [1] predicts that prestressing would very substantially increase the shear capacity of the beams. Beam SP3 is predicted to be 91% stronger than Beam SP0. The compression field theory predicts a more moderate gain in shear strength with prestress with Beam SP3 being predicted to be 29% stronger than SP0.

The experimental results showed that prestressing indeed increased the shear capacity, Fig. 7, so that Beam SP3 was 31% stronger than Beam SP0. While the trend of the experimental results was accurately predicted by the compression field theory the actual shear strengths were considerably in excess of the predictions. This was partly due to the conservative nature of the empirical stress limit, Eq.(2), and may also have been caused by end restraint of the test specimens [12].

7. CONCLUDING REMARKS

The research programme summarized in this paper has not yet resulted in a unified beam theory capable of predicting the behaviour of any reinforced concrete cross-section under any combination of loading. It is, however, believed that significant progress has been made in achieving this ultimate objective.

At present predictions for members subjected to complex loading (say all six stress resultants simultaneously) can be made with the aid of truss analogies [13], and automatic design programmes based on such analogies [14] are in use. These models, however, involve empirical assumptions as to what are the effec-

tive areas of the various components of the truss and hence they are not comparable to the "plane sections" theory for flexure which remains the "standard" against which we wish to judge all other theories.

ACKNOWLEDGEMENTS

The research reported in this paper was made possible by a series of grants from the Natural Science and Engineering Research Council of Canada. This continuing support is gratefully acknowledged.

REFERENCES

1. ACI: Building Code Requirements for Reinforced Concrete (ACI 318-77), ACI Detroit, 1977
2. PARK,R., PAULAY,T.: Reinforced Concrete Structures, John Wiley,New York 1975
3. MITCHELL,D, COLLINS,M.P.: Diagonal Compression Field Theory - A Rational Model for Structural Concrete in Pure Torsion, ACI Journal, Vol.71, Aug. 1974, pp. 396-408
4. ONSONGO,W.M.: The Diagonal Compression Field Theory for Reinforced Concrete Beams Subjected to Combined Torsion, Flexure and Axial Load, thesis presented to University of Toronto, Toronto, Canada, in 1978, in partial fulfillment of the requirements for the degree of Doctor of Philosophy
5. COLLINS,M.P.: Towards a Rational Theory for RC Members in Shear, Journal of the Structural Division, ASCE, Vol. 104, April 1978, pp. 649-666
6. COLLINS,M.P.: Reinforced Concrete in Flexure and Shear, Proceedings of the Mark W. Huggins Symposium on Structural Engineering, University of Toronto, September 1978
7. COLLINS,M.P.: Investigating the Stress-Strain Characteristics of Diagonally Cracked Concrete, IABSE Colloquium on Plasticity in Reinforced Concrete, Copenhagen, May 1979
8. LAMPERT,P., THUERLIMANN,B.: Ultimate Strength and Design of Reinforced Concrete Beams in Torsion and Bending, IABSE, Publication 31-I, 1971 pp107-131
9. NIELSEN,M.P., BRAESTRUP,M.W.: Plastic Shear Strength of Reinforced Concrete Beams, Bygningsstatiske Meddelelser, Copenhagen, Vol.46,No.3,1975,pp 61-99
10. HSU,T.T.C.: Torsion of Structural Concrete - Behavior of Reinforced Concrete Rectangular Members, Torsion of Structural Concrete, SP-18, ACI, Detroit, 1968, pp. 261-306
11. CEB-FIP, Model Code for Concrete Structures, Comité Euro-International du Béton, Bulletin d'Information No. 125-E, Paris, April 1978
12. SADLER,C.: Investigating Shear Design Criteria for Prestressed Concrete Girders, thesis presented to University of Toronto, Toronto, Canada, in 1978, in partial fulfillment of the requirements for the degree of Master of Applied Science
13. RABBAT,B.G., COLLINS,M.P.: A Variable Angle Space Truss Model for Structural Concrete Members Subjected to Complex Loading, ACI, Douglas McHenry International Symposium on Concrete and Concrete Structures, ACI SP-55, 1978 pp. 547-587
14. RABBAT,B.G., COLLINS,M.P.: The Computer Aided Design of Structural Concrete Sections Subjected to Combined Loading, Computers and Structures, Vol. 7, No. 2, Permagon Press, April 1977, pp. 229-236

Additional remark to pure torsion

HEES, G.

We tested bars with rectangular crosssections / 1 / and relations b/d from 1/1 to 1/8. In the last case, there is an inner region (lying between the dashed lines) which can be regarded as a plate with constant main bending moments in the direktion of 45°. The calculated stresses and deformations of this bending bars and the measured ones were nearly equal. If we changed the thicknes of the walls in the box-girder-modell of Lampert a little bit we calculated the same values. In the outer regions are difficult stress relations and at the moment I am not able to describe this problem. – If the relation of b/d is greater than 1/3, the influence of the outer regions increases and therefore it is not possible to calculate bending bars. But also the box-girder-modell is not full satisfactory.

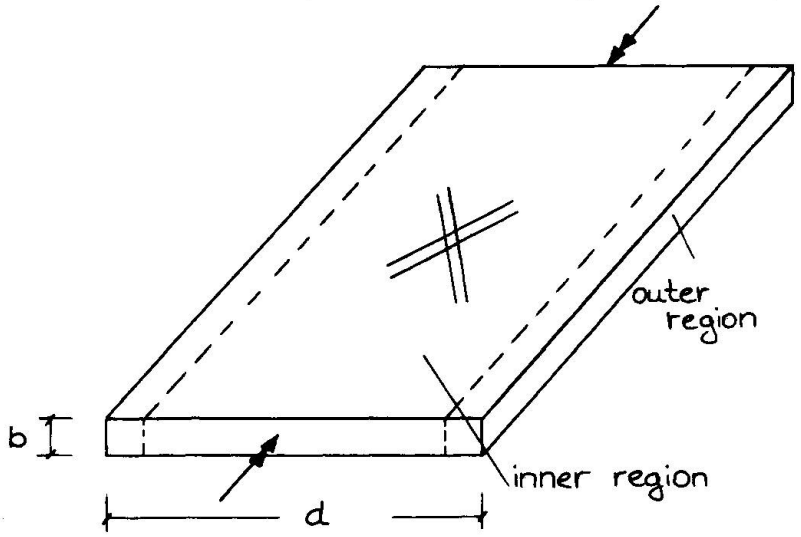

/ 1 / Kraft, U.: Ermittlung des Torsionstragverhaltens von Stahlbetonbalken und Stahlbetonplatten mit Microbetonmodellen, Universitätsbibliothek der TU Berlin, Abteilung Publikation, D 1000 Berlin 12

SUMMARY OF DISCUSSION - SESSION 2

1. Limit State Design

With ambitious hopes for the future of plastic analysis as a means of structural design, B. Thürlimannn had opened his introductory lecture on "Plastic Analysis of Reinforced Concrete Beams" with a picture of the free cantilever construction method being applied to a major prestressed box girder bridge.

J. Blaauwendraad profited from this example to question rhetorically the value of plastic analysis in treating the major design problems encountered in the actual design of such structures. As pointed out, the cross section may be multicellular with cantilever flanges and not the academic rectangular boxes which form the basis for the theory. Also the multitude of prestressing cables needed in such a structure leads to considerable organisational problems in reaching a satisfactory positioning of the cables within the geometric restraints of the cross sections.

Further a major problem in designing such structures is the control of the horizontal alignment and of the short- and long term deflections, in order to ensure the required form of the finished structure. B. Thürlimann replied that of course plastic analysis could not treat serviceability requirements.

In this way B. Thürlimann focused on the important fact that plastic analysis is a rational means of treating the ultimate limit state conditions only. To achieve a fully operational design basis, plastic analysis should be supplemented by other analytical methods able to treat the requirements within the serviceability limit states.

When developing a complete design basis, this dualism, reflecting modern design principles, should not be forgotten.

2. Basics of Plastic Design

The further discussion focused on some of the basic problems still to be dealt with in some detail before a broad acceptance of the modern rational theory of plasticity can be achieved.

B. Thürlimann drew attention to the multitude of different effects covered by the effectiveness factor ν. Effects such as stress concentrations at the intersection between stirrups and longitudinal reinforcement, effective wall thickness in box- or solid cross sections subjected to torsion, distorsion of the side walls of such box sections, and bond slip are just a few examples of the role of ν. B. Thürlimann therefore recommended that much care should be exerted in defining what was covered by ν, so as possibly to separate the different effects caused by ν. In this way a rational explanation of the origin of the ν - values could answer for the different values of ν presented for each type of test. The criticism that ν is often just an empirical calibration factor introduced to improve the relation between theoretical and experimental results, could be dealt with in a more satisfactory manner.

Contrary to this opinion, M.W. Braestrup felt that the problem was more to make a choice of the values for ν than to make a calculation of ν. The code could specify the values to be used in the different types of load effects, as this

is already done in several cases - just using another terminology than "effectiveness factor", e.g. maximum concrete compression design strength being different in bending, shear and torsion.

J. Witteveen discussed the deformability of concrete fundamentally necessary for the application of lower and upper bounds in plastic theory. Extensive research on plates has shown that in the yield lines considerable rotation can take place under a constant or even slightly increasing moment. According to Witteveen, the contributions on reinforced concrete shear walls and beams presented so far at this Colloquium have given no proof that concrete in compression has adequate deformation capacity for these structural elements to indeed reach the plastic collapse load. After a certain deformation, concrete in compression "softens", while it is well known from the plastic theory of steel structures that "hardening" in Witteveen's terms is essential for the formation of plastic zones. This strain softening of concrete in compression is taken into account by introducing the effectiveness factor ν. Also J. Witteveen therefore found that the fundamental weakness of the approach was the fact that ν depends on many factors such as the type of structure, type of loading, type of statically admissible stress field chosen, and the type of failure mechanism.

The freedom achieved with plastic analysis to choose the statically admissible stress field and design accordingly has of course its price, but as pointed out by B. Thürlimann the answer to this question depends on the case considered. When, for example, applying the plastic hinge approach to design a frame, the necessary rotation capacity of the hinges, and thus the necessary deformation capacity of the concrete, depends completely on whether all hinges form at the same time or whether there is a substantial difference in load level between the formation of the first hinge and the last hinge. The experience, as expressed by Thürlimann, is that concrete has a formidable ability to redistribute stresses, and if the effective concrete compression strength is applied sensibly, the design proves to be satisfactory.

The discussion on the origin and role of the ν -factor was concluded by referrring to the paper by H. Exner, "On the Effectiveness Factor in Plastic Analysis of Concrete" presented in Session 1, this theme being a central subject within the theory of plastic analysis of concrete and a field in which further research should be encouraged.

3. Shear

A. Losberg discussed the possible influence of prestressed reinforcement on the shear capacity of beams in plastic design. The preliminary results of ongoing shear tests on simply supported beams with one cantilever, representing the support region of continuous beams, was reported. The parameters varied were the level of prestress and the existence or non-existence of stirrups in the shear failure region behind the support near the cantilever. Furthermore the prestressed reinforcement was in some of the test beams brought to yield by external stressing just prior to shear failure in order to study the possible decreased or vanishing effect of prestress upon the shear carrying capacity when the prestressed main reinforcement yields prior to a shear failure.

According to Losberg, the test results show that the level of prestress has a considerable influence on the shear carrying capacity, and that this effect could be fully represented by an influence term of the traditional type.

Furthermore there was no significant difference between the shear capacity of beams with yielding support reinforcement and with non-yielding support reinforcement.

Based on the contribution on "Shear in Beams with Bent-Up Bars" by C.M. Pedersen, A. Losberg noted that the effect of bent-up bars now seemed to be better considered than previously. To Losberg's question on whether separate methods were required to treat the effect of stirrups and of bent-up bars, Pedersen reported that all the tests he had studied verified the theoretically predicted result that there is no basic difference in the ability of stirrups and of bent-up bars to carry shear, and that a distinction is thus unwarranted.

B.C. Jensen pointed out that the model applied by J.F. Jensen to treat the lower bound shear strength of non-shear reinforced beams required that either the longitudinal support reinforcement be situated half-way up the support zone under two-dimensional hydrostatic pressure to ensure equilibrium, or a longer support region would be needed to ensure adequate stress transfer between the longitudinal reinforcement and the inclined uniaxial stress zone. J.F. Jensen found that an additional moment transfer system at the support zone could easily be achieved either by the concrete itself or supplemented by a few additional stirrups behind the support region.

Another possibility, shown by P. Marti, was to introduce a stress field for the part of the beam behind the support, which may for example be constructed starting from a simple truss model. In this case a certain stirrup reinforcement behind the support as well as a longitudinal reinforcement in the upper part - or at the top of the beam - will be needed. In any case, a simple bending failure mechanism may possibly be associated with an inclined collapse crack beneath the centre of rotation.

4. Statically Admissible Stress Field

P. Marti also reminded the gathering that the problems of simply supported rectangular beams under concentrated and uniformly distributed loads have already been treated by D.C. Drucker in his 1961 IABSE article "On Structural Concrete and the Theorems of Limit Analysis". In this article Drucker showed that in these cases a compatible bending failure mechanism may always be associated with the statically admissible stress field. According to Marti, the same remark also applies to the class of complete solutions given by M.P. Nielsen in his dissertation "On the Strength of Reinforced Concrete Discs".

S. ROSTAM